Università Degli Studi Di Napoli Federico II

PhD in Chemical Sciences

XXVIII Cycle

Biological function of D-Aspartate in the mammalian brain

PhD Student:

Marta Squillace

Tutor:

Prof. Piero Pucci

Indice

1.Introduction……3

1.1 D-Amino acids in mammalian tissue……..…….....3

1.2 D-Aspartate in mammals ……...……..4

1.3 Regulation of D-Aspartate levels in mammalian brain …….....5

1.4 Pharmacological influence of D-aspartate on NMDAR-dependent transmission……...7

1.5 Release and uptake of D-Aspartate ……10

1.6 Schizophrenia, NMDARs and D-amino acids ……11

1.7 Mouse models with deregulated higher levels of D-aspartate……13

1.8 Influence of increased D-aspartate levels on striatal synaptic plasticity and sensorimotor gating…….....…….....13

2.Aim of the research……15

3.Results……16

3.1 D-aspartate levels in the post-mortem prefrontal cortex and caudate putamen of schizophrenia patients…….……16

3.2 Expression of NMDAR subunits are selectively reduced in the *post-mortem* prefrontal cortex of schizophrenia patients...…….……...18

3.3 DDO mRNA expression and methylation of the DDO gene in the *post mortem* SCZ brain……...……...19

3.4 LC/MSMS in *Ddo*$^{-/-}$……20

3.5 Dendritic morphology in mice with high levels of D-Aspartate .……23

3.6 High levels of D-Asp converts E-LTP into L-LTP in the adult hippocampus ……....26

3.7 Increased levels of D-Asp affect schizophrenia-like behavior induced by PCP in mice……...……28

3.8 fMRI response induced by PCP ……..31

3.9 Does D-Asp cross the blood brain barrier?.....33

3.10 D-Asp is released in a calcium-dependent manner……34

3.11 D-Asp modulates L-Glutamate release in the mouse brain…….36

3.12 Effect of olanzapine on L-Glutamate, D-Aspartate and L-Aspartate extracellular levels……...38

3.13 Effect of Olanzapine on DDO activity……39

4.Conclusion……41

5.Materials and Methods……..46

5.1 Tissue collection……46

5.2 HPLC analysis on human samples……46

5.3 Western blotting……48

5.4 Quantitative reverse transcription-polymerase chain reaction analysis in humans……..50

5.5 Methylation analysis……...……..51

5.6 Animals……...……..52

5.7 LC-MS/MS……...……53

5.8 Golgi-Cox staining and dendritic spine measurements……54

5.9 Electrophysiology……...……..55

5.10 PCP-induced motor activity……...…….56

5.11 Prepulse inhibition of the startle reflex under PCP treatment…….56

5.12 Functional and pharmacological magnetic resonance imaging...……56

5.13 *In vivo* microdialysis……...…….57

5.14 High-performance liquid chromatography analysis……...….58

5.15 Synaptosomes preparation……...……....59

5.16 Enzymes and inhibition assays ……....60

6.Bibliography……..61

7. Pubblications……..74

1. Introduction

1.1 D-Amino acids in mammalian tissue

Every amino acid (except glycine) can occur in two isomeric forms, because of the possibility of forming two different enantiomers (stereoisomers) around the central carbon atom. By convention, they are called L- and D- forms, analogous to left-handed and right-handed configurations (Figure 1).

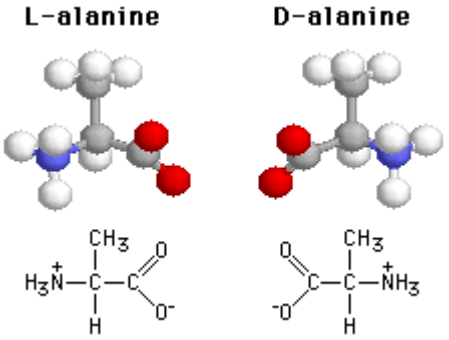

Figure 1.1: example of D- and L- form of amino acids

Only L-amino acids are manufactured in cells and incorporated into proteins. Some D-amino acids are found in the cell walls of bacteria, thus conferring protection against attacks of protease and microorganisms (Corrigan, 1969). D-amino acids are incorporated into the peptides via two different mechanisms. The first mechanism is post-translational conversion of L- to D-amino acids within peptides that were originally synthesized in ribosomes. The second mechanism requires the activity of non-ribosomal peptide (NRP) synthetases, which, unlike ribosomal peptide synthesis, generates peptides independent of messenger RNA. While posttranslational modification occurs primarily in eukaryotes, NRP synthesis is more frequent in bacteria (Cava et al., 2011). In mammals, D-amino acids have only been detected in metabolically inert proteins owing to processes of spontaneous racemization occurring with age (Fujii, 2002, 2005). Therefore, for many years it was commonly assumed that only L-amino acids have a biological role in mammals. However, in the years 80-90 the refinement of sensitive analytical techniques revealed appreciable concentrations of free D-amino acids, such as D-serine (D-Ser) and D-aspartate (D-Asp), in the brain

and peripheral organs of rodents and man (Dunlop et al., 1986; Hashimoto et al., 1992b; Hashimoto et al., 1992a).

1.2 D-Aspartate in mammals

The presence of endogenous free D-Asp has been described in mammals such as mouse, rat and human, starting from the mid-80s (Dunlop et al., 1986; Neidle and Dunlop, 1990; Hashimoto et al., 1993). D-Asp is present both in the central nervous system and endocrine glands, appearing with a peculiar temporal occurrence pattern. In endocrine glands, D-Asp content increases during post-natal and adult phase, in concomitance with their functional maturation, hence the appearance of this D-amino acid has been functionally correlated with the synthesis and/or the release of different hormones (Furuchi and Homma, 2005; D'Aniello, 2007). In contrast to peripheral organs, transient occurrence of D-Asp has been demonstrated in the brain, where it is selectively found at very high concentrations during embryo and perinatal phases (Dunlop et al., 1986; Neidle and Dunlop, 1990; Hashimoto et al., 1993; Hashimoto et al., 1995; Sakai et al., 1998; Wolosker et al., 2000).. Localization of D-Asp was analyzed throughout the first post-natal month of life (Wolosker et al., 2000) (Figure 1.2). Between post-natal day 0 (P0) and P2, D-Asp was found at considerable levels in the forebrain and midbrain, and then also in the caudal-most regions of the brain. At these perinatal stages, D-Asp is concentrated in neuronal sets of the cerebral cortex, hippocampus and cerebellum, which are actively involved in developmental processes. At P7, D-Asp immunostaining uniformly decreases in the brain, to almost disappear at P28.

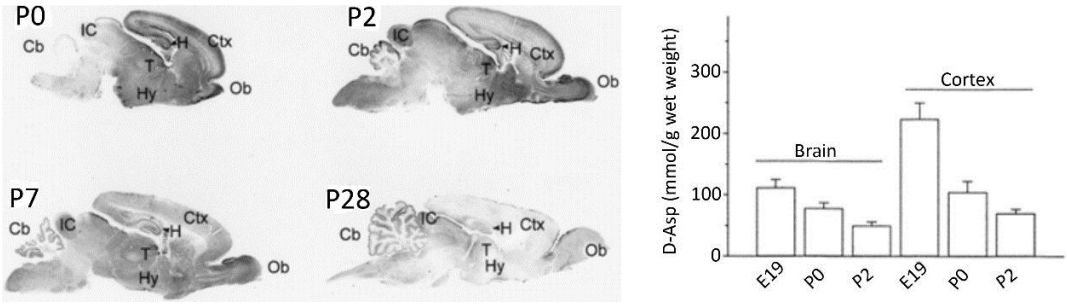

Figure 1.2: Localizations of D-Asp during postnatal development. Left Panel: D-Asp was localized by immunohistochemistry. At P0, highest levels are observed in the cerebral cortex (Ctx), olfactory bulb (Ob) and hippocampus (H). At P2, staining increases in the cerebellum (Cb) and inferior colliculi (IC), while levels remain unchanged in the hypothalamus (Hy) and olfactory bulb. Overall levels of D-Asp decrease at P7 and P28. Right panel: D-Asp were measured by HPLC in total rat brain and cerebral cortex.

One important point to keep in mind is that at all phases and in all brain areas, D-Asp is exclusively restricted to neuronal population, localized both in cytoplasm and fiber tracks, without any evident staining in glia (Schell et al., 1997; Wolosker et al., 2000). Surprisingly, HPLC analysis performed on prefrontal cortex (PFC) homogenates from fetuses unveiled that D-Asp amount at gestational week 14 even exceeds that of the corresponding L-form (Hashimoto et al., 1993). It is noteworthy to highlight that in neurosecretory neurons of the rat hypothalamus, D-Asp has been detected in the nucleoli, in close association with heterochromatin (Wang et al., 2002). This observation prompted authors to hypothesize that this D-amino acid may be involved also in the control of gene expression (Wang et al., 2002).

1.3 Regulation of D-Aspartate levels in mammalian brain

The specific temporal and regional changes of D-Asp contents in mammalian tissues imply the existence of biochemical mechanisms for the precise modulation of its endogenous levels. On the other hand, the supposed derivation of D-Asp from exogenous sources, such as the diet, or from endogenous metabolically stable proteins cannot explain the prenatal peak of occurrence of this D-amino acid in the brain. In this regard, time-dependent accumulation of D-Asp in D-Asp-free pheochromocytoma PC12 cells (Long et al., 1998), and conversion of [C^{14}]L-Asp into [C^{14}]D-Asp in primary neuronal cell cultures from rats (Wolosker et al., 2000) suggested that this D-amino acid can be autonomously synthesized in mammalian cells, via a putative Asp racemase enzyme (Homma, 2007; Katane and Homma, 2011). A few years ago, a mouse pyridoxal 5'-phosphate (PLP)-dependent glutamate-oxalacetate transaminase 1-like 1 (Got1l1), which substantially converts L-Aspartate (L-Asp) to D-Asp and colocalizes with D-Asp in the adult brain, has been identified as the main source of endogenous D-Asp in this organ (Kim et al., 2010). On the other side, a recent publication has demonstrated that Got1l1 mRNA is undetectable in the brain. Moreover, the recombinant enzyme shows L-Asp aminotransferase activity but lacks Asp racemase activity. In agreement with biochemical results, knockout mice for *Got1l1* display D-Asp levels comparable to those of wild-type animals (Tanaka-Hayashi et al., 2014) suggesting there might be an as yet unknown enzyme for D-Asp synthesis. Interestingly, another study has evidenced that D-Asp levels are reduced in

the forebrain of serine racemase knockout mice (*Srr*-KO) (Horio et al., 2013), thus suggesting a novel potential unexpected pathway for the generation of D-Asp in the brain or that the synthesis of D-Asp is directly related to D-Ser production in the brain. If the biosynthesis of D-Asp is still a controversial topic, the existence of an enzyme catabolising free D-Asp, D-aspartate oxidase (DDO, EC 1.4.3.1), has long been established (Still et al., 1949). DDO is a flavin adenine dinucleotide (FAD)-containing flavoprotein (Van Veldhoven et al., 1991) which oxidizes D-Asp in presence of H_2O and O_2, producing α-oxaloacetate, H_2O_2 and NH_4^+ ions (D'Aniello et al., 1993) (Figure 1.3).

Figure 1.3: conversion of D-Asp in α-oxaloacetate by D-aspartate oxidase (DDO).

Besides D-Asp, DDO is able to selectively oxidize *in vitro* also other bicarboxylic D-amino acids, such as D-glutamate (D-Glu) and N-methyl D-aspartate (NMDA), while it is inactive towards all the other D-amino acids including D-Ser (Setoyama and Miura, 1997), that are degraded by the D-amino acid oxidase (DAAO, EC 1.4.3.3), a flavoenzyme homologous to DDO (Negri et al., 1992; Pollegioni et al., 2007; Sacchi et al., 2012). The protein sequence possesses a functional C-terminal tripeptide for the targeting to peroxisomes (Setoyama and Miura, 1997; Amery et al., 1998), where DDO is supposed to oxidize D-Asp and release its catabolites (Beard, 1990). Localization of this enzyme into catalase-containing organelles like peroxisomes allows the cell to safely remove H_2O_2, a toxic product of D-amino acids metabolism (Katane and Homma, 2010). In the brain, DDO is expressed at post-natal phases since its activity strongly increases from birth until 6 weeks of life (Van Veldhoven et al., 1991) (Figure 1.4), and is predominantly localized in neuronal population (Zaar et al., 2002). The onset of DDO activity after birth and its progressive increase imply a control of this enzyme on the postnatal levels of D-Asp. However, it has been unclear for long time whether time-dependent activity of DDO correlates with *Ddo* gene expression. In this regard, recent finding in mice indicates that the gradual decrease of D-Asp content, in a time-window between E15 and P60, is accompanied by complementary increased

transcription of *Ddo* gene (Punzo et al., 2016), thus matching with the previously reported enhanced postnatal DDO activity (Van Veldhoven et al., 1991). Interestingly, the temporal postnatal increase in *Ddo* mRNA levels is reflected by progressive demethylation in the CpG sites of *Ddo* surrounding the transcription start site (8 CpG residues from -363 to +113 bp). This observation seems to have functional impact on *Ddo* gene transcription since treatment with the demethylating agent azacitidine is able to substantially trigger *Ddo* transcription in primary neuronal cultures from embryonic cortex that, normally, do not express the gene (Punzo et al., 2016). In agreement with a physiological activity of DDO over endogenous free D-Asp, histochemical detection in the rat brain shows that DDO expression is reciprocal to D-Asp localization (Schell et al., 1997).

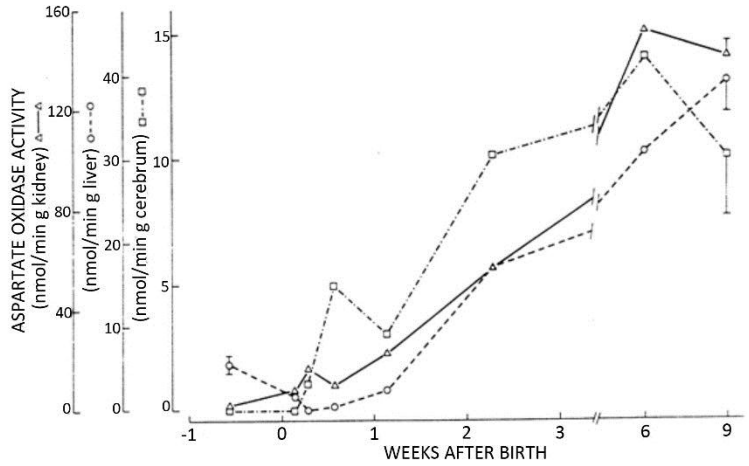

Figure 1.4: DDO activity during postnatal life in kidney, liver and cerebrum

1.4 Pharmacological influence of D-aspartate on NMDAR-dependent transmission

NMDA subclass of ionotropic glutamate (Glu) receptors has generated for a long time an enormous interest in neuroscience due to its implication in developmental and physiological neuronal processes (Ikonomidou et al., 2001; Ritter et al., 2002; Nacher and McEwen, 2006). In addition, alterations in NMDARs activity have also been reported in neuropathological disorders including epilepsy, Alzheimer's disease and schizophrenia (SCZ) (Javitt, 2004; Kalia et al., 2008; Nistico et al., 2012). NMDA receptors (NMDARs) are composed of GluN1subunit combined with the different four

GluN2 subunits (A-D), where the functional properties of each heteromeric assembly strictly depend on the specific subunit composition (Cull-Candy and Leszkiewicz, 2004). The NMDAR ion channel is permeable to monovalent cations, including Na^+ and K^+ and divalent cations, most notably Ca^{2+}. Moreover, there is a binding site within the channel pore for Mg^{2+}. At resting membrane potential, Mg^{2+} binds to this site largely blocking ion flow through the channel. When the membrane is depolarized, Mg^{2+} is expelled from the channel allowing for greatly enhanced passage of ions. Activation of NMDAR leads to Ca^{2+} currents which overall are able to trigger several complex intracellular responses, including the activation of guanylate cyclase, release of arachidonic acid, translocation and activation of protein kinase C and modulation of gene expression (Dingledine et al., 1999; Hardingham and Bading, 2010).

In the past decades, a considerable number of studies have investigated the molecular binding between the different subclasses of L-Glu receptors and various L-Glu analogues with potential ligand affinity, in order to find new pharmacological agents with agonistic or antagonistic activity. Among these compounds, D-Asp emerged as a molecule able to bind NMDARs, owing to a relatively high affinity for their Glu binding site (Fagg and Matus, 1984; Monahan and Michel, 1987; Ogita and Yoneda, 1988; Olverman et al., 1988; Ransom and Stec, 1988). A comparative binding study in rat brain membranes demonstrated that the potency of D-Asp to displace the binding of the competitive NMDAR antagonist, [H^3]AP5, is the same of NMDA and 10-fold lower than L-Glu (Olverman et al., 1988). In agreement with these *in vitro* binding assays, voltage-clamp recordings from CA1 pyramidal neurons in mouse hippocampal slices indicate that local applications of D-Asp are able to induce inward currents, antagonized in a concentration-dependent and reversible manner by competitive and non-competitive blockers of NMDARs, such as D-AP5 and MK-801, respectively (Errico et al., 2008b) (Figure 1.5).

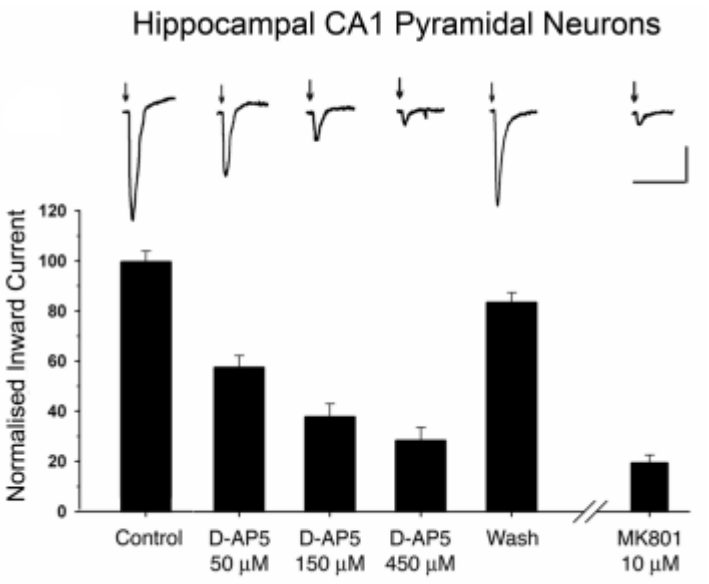

Figure 1.5: Inward currents recorded from CA1 pyramidal neurons of Ddo+/+ mice following local pressure application of D-aspartate (arrows), are reduced by D-AP5 in a concentration-dependent and reversible manner, and persistently diminished by MK801 (10 µM).

However, as shown in figure, both antagonists used do not completely reset the current induced by D-Asp. Interestingly, residual D-Asp-dependent currents still persist also after the simultaneous perfusion of selective antagonists of NR2A, NR2B and NR2C-D subunits of NMDARs or even after the application of high concentrations of D-AP5 or MK-801 (Errico et al., 2008b; Errico et al., 2011b; Errico et al., 2011a), thus suggesting the existence of NMDAR-independent currents triggered by this D-amino acid. In this respect, it has been shown that D-Asp is able to inhibit kainate-induced AMPA receptor currents in acutely isolated rat hippocampal neurons (Gong et al., 2005). Another study indicates that D-Asp can also activate mGluR5 receptors, coupled to polyphosphoinositide hydrolysis, in neonate rat hippocampal and cortical slices (Molinaro et al., 2010). Likewise, a recent study performed in dopamine neurons of the *substantia nigra pars compacta* of mice has shown that currents produced by D-Asp are mainly dependent by NMDAR but a smaller component is also mediated by ionotropic AMPA receptors and metabotropic Glu1/5 receptors (Krashia et al., 2015). These observations expand the range of potential targets for D-Asp action, although the origin of the NMDAR-independent currents stimulated by D-Asp remains to be further clarified.

1.5 Release and uptake of D-Aspartate

If D-Asp is actually able to mediate intercellular communication in the brain by influencing NMDAR-dependent transmission, then there should be a mechanism to allow also the extracellular release and the subsequent reuptake of this D-amino acid. Experiments using radiolabeled D-Asp in rat brain slices demonstrated that intracellular D-Asp is released upon chemical and electrical stimulation (Savage et al., 2001). The release of D-Asp to the extracellular environment has been measured from D-Asp-containing tissues or cells of the mammalian brain in a Ca^{2+}-dependent manner (Davies and Johnston, 1976; Malthe-Sorenssen et al., 1979; Nakatsuka et al., 2001). The relevant role of Ca^{2+} for triggering D-Asp release was unequivocally demonstrated in experiments using chelating agents for Ca^{2+}, able to strongly reduce D-Asp efflux after exposure to KCl (Wolosker et al., 2000). Besides to a Ca^{2+}-dependent release, other studies suggest that also L-Glutamate (L-Glu) transporters may contribute to the efflux of intracellular D-Asp via heteroexchange mechanism, as observed in cultures of mouse neurons and astrocytes (Anderson et al., 2001; Bak et al., 2003). In addition, spontaneous D-Asp release, that is independent of Ca^{2+}-related exocytosis, has also been reported (Adachi et al., 2004; Koyama et al., 2006).

Presynaptic nerve terminals express L-Glu/L-Asp transport systems that utilize a Na^{+}-dependent mechanism to move excitatory L-amino acids against their concentration gradient. The first reports showing high and specific affinity of D-Asp for L-Glu transporters (excitatory amino acids transporters, EAATs) came from studies on the characterization of transporter systems by means of radiolabeled uptake ligands (Davies and Johnston, 1976; Streit, 1980; Storm-Mathisen and Wold, 1981; Wilkin et al., 1982; Taxt and Storm-Mathisen, 1984). Subsequent investigations following the isolation and cloning of EAAT subtypes have confirmed that all of them are able to transport L- and D-Asp in a stereoblind fashion (Palacin et al., 1998).

Besides the *in vitro* results reported above, the prerequisite to sustain that D-Asp is physiologically involved in NMDAR-related neurotransmission is the demonstration that this D-amino acid occurs in the *in vivo* brain at extracellular level, where it can actually stimulate the target receptor. This evidence has recently turned out from a microdialysis study demonstrating that D-Asp is present at nanomolar concentrations in the extracellular space of the prefrontal cortex of freely moving mice (Punzo et al.,

2016). Interestingly, when dialysate fraction is collected in a Ca^{2+}-free artificial cerebrospinal fluid (ACSF), extracellular D-Asp levels become undetectable, suggesting that D-Asp is released in a Ca^{2+}-dependent manner and that the pre-existing D-Asp has been efficiently removed from the extracellular space (Punzo et al., 2016). Moreover, the lack of DDO in *Ddo* knockout mice (*Ddo*$^{-/-}$) (Errico et al., 2006) leads to the concomitant increase of extracellular and total D-Asp content in the PFC, indicating that impaired catabolism of D-Asp affects the extracellular release of this D-amino acid (Punzo et al., 2016).

1.6 Schizophrenia, NMDARs and D-amino acids

Schizophrenia (SCZ) is a chronic, severe, debilitating mental illness that affects about 1% of the population and generally appears in late adolescence or early adulthood. In many cases the disorder develops so slowly that the sufferer does not know he/she has it for a long time. With other people it can strike suddenly and develop fast. It is considered to be the result of a complex group of genetic, psychological, and environmental factors. SCZ is often described in terms of positive and negative symptoms. Positive symptoms are those that most individuals do not normally experience but are present in people with schizophrenia. They can include delusions, disordered thoughts and speech, and tactile, auditory, visual, olfactory and gustatory hallucinations, typically regarded as manifestations of psychosis. Positive symptoms generally respond well to medication. Negative symptoms are deficits of normal emotional responses or of other thought processes, and respond less well to medication. They commonly include flat or blunted affect and emotion, poverty of speech (alogia), inability to experience pleasure (anhedonia), lack of desire to form relationships (asociality), and lack of motivation (avolition). Of the many contemporary theories of SCZ, the most enduring has been the dopamine hypothesis. It is based on knowledge of antipsychotic medications, as well as the effects of illicit substances such as amphetamines: under the influence of amphetamine the brain is flooded with dopamine and norepinephrine and amphetamine-induced psychosis closely resembles paranoid SCZ. Using these facts as a starting point, scientists figured out that patients with SCZ have excessive dopamine receptors in specific brain regions.

On the other hand, glutamatergic models of SCZ were first proposed approximately 20 years ago (Javitt, 1987), based on the early observation that phencyclidine (PCP), ketamine, and related drugs induced SCZ-like psychotic effects, followed later by the observation that these compounds induce their unique behavioral effects by blocking neurotransmission at NMDARs (Javitt and Zukin, 1991). Since that time, neurochemical models based on actions of PCP and ketamine have become increasingly well established, with focus on glutamatergic dysfunction as a basis for both symptoms and cognitive dysfunction in SCZ. Accordingly, facilitation of NMDAR-mediated neurotransmission has been proposed as a strategic therapeutic approach in SCZ. Consistent with this idea, several reports have demonstrated the clinical benefits of targeting the glycine binding-site of the NMDARs (Coyle et al., 2002; Millan, 2002). Nowadays, D-Ser, D-cycloserine and glycine are the most promising molecules in SCZ treatment, given their ability to bind and activate this site (Cascella et al., 1994; Javitt et al., 1994; Goff et al., 1995; Tsai et al., 1998; Heresco-Levy et al., 2002; de Bartolomeis et al., 2012). In particular, the clinical interest for D-Ser has been supported by altered D-Ser metabolism in SCZ patients. In this regard, Hashimoto and coworkers found lower concentrations of D-Ser in serum of patients with SCZ (Hashimoto et al., 2003). Together with D-Asp, D-Ser is the only D-amino acid present at high concentrations in the mammalian brain (Hashimoto and Oka, 1997). This D-amino acid is generated by the activity of the pyrodoxal 5-phosphate-dependent serine racemase enzyme (SR) (Wolosker et al., 1999) and its degradation occurs via the activity of peroxisomal flavoprotein D-amino acid oxidase (DAAO) (Krebs, 1935). To support the neurobiological and clinical interest of this unconventional D-amino acid in SCZ physiopathology, genetic and functional studies report that the *DAAO* gene is a marker of susceptibility to SCZ (Labrie et al., 2012).
Based on the aforementioned observations and considering that also D-Asp, by binding glutamate-binding site, acts on the NMDARs as an endogenous agonist, we hypothesized that also this D-amino acid may play a role in SCZ.

1.7 Mouse models with deregulated higher levels of D-aspartate.

In order to comprehend the *in vivo* function of D-Asp and of its catabolic enzyme DDO, in the last years a knockout mouse model have been generated through the targeted deletion of the *Ddo* gene (Errico et al., 2006). Measurement of endogenous free D-Asp levels by HPLC in the whole brain and in peripheral organs of knockout line (*Ddo*$^{-/-}$) have revealed a strong increase of this D-amino acid, compared to respective wild-type littermates, while no difference between genotypes was found in the content of bicarboxylic L-amino acids, L-Asp (Errico et al., 2006; Huang et al., 2006) and L-Glu (Huang et al., 2006). A more detailed neurochemical evaluation in specific brain regions of *Ddo*$^{-/-}$ mice, like the hippocampus, caudate putamen, cortex, cerebellum and olfactory bulbs, has confirmed that D-Asp increases approximately 10- to 20-fold, in relation to the corresponding wild-type brain areas (Errico et al., 2008b; Errico et al., 2008a; Errico et al., 2011c). Interestingly, as a direct consequence of D-Asp increase, *Ddo*$^{-/-}$ brains also display higher content of endogenous NMDA (Errico et al., 2006; Errico et al., 2011c), the N-methyl derivative of D-Asp.

Besides *Ddo* gene targeting, an alternative approach has been developed to increase D-Asp levels, based on 1- or 2-months-oral administration of D-Asp delivered in drink water to C57BL/6 mice. In this mouse model, HPLC detection has revealed a significant increase of D-Asp levels in the brain, even though to a lesser extent than in *Ddo*$^{-/-}$ animals due to the presence of DDO enzyme. Indeed, depending on the brain region examined and on the schedule of D-Asp administration, the endogenous levels of D-Asp in the hippocampus, cortex, caudate putamen and cerebellum of treated animals increase approximately from 2- to 5-fold, compared to the same brain areas of untreated mice (Errico et al., 2008b; Errico et al., 2008a; Errico et al., 2011b).

1.8 Influence of increased D-aspartate levels on striatal synaptic plasticity and sensorimotor gating.

Evaluation of electrophysiological properties of D-Asp in the caudate putamen indicates that local applications of this D-amino acid induce dose-dependent inward currents that, similarly to the hippocampus, are antagonized by the NMDAR blockers

MK801 and D-AP5 (Errico et al., 2008a). The effect of D-Asp on striatal glutamatergic transmission has been also extensively studied in *Ddo*$^{-/-}$ and D-Asp-treated mice. Electrophysiological data indicate that the excess of D-Asp is able to completely abolish corticostriatal long-term depression (LTD) (Errico et al., 2008a) and depotentiation (Errico et al., 2011c). Given the ability of D-Asp to activate striatal NMDARs, it is likely that the absence of corticostriatal LTD, in conditions of enhanced levels of D-Asp, may depend on the facilitatory effect of this D-amino acid on NMDAR-dependent transmission (Calabresi et al., 1992; Centonze et al., 2007). The effect of increased D-Asp on striatal LTD deserves a special remark if we consider that similar synaptic adaptations occur after chronic treatment with the typical antipsychotic haloperidol (Centonze et al., 2004). Moreover, *in vivo* experiments of acoustic startle response and prepulse inhibition (PPI), a test used to evaluate schizophrenia-like behaviour, indicate that chronic exposure to higher D-Asp levels does not affect basal properties of sensorimotor filtering but significantly attenuates the psychotic-like deficits induced in mice by the treatment with the psychotomimetic drugs amphetamine and MK801 (Errico et al., 2008a). Altogether, these data suggest a potential beneficial effect of D-Asp on sensorimotor filtering abilities.

2. Aim of the research

Increasing evidence points to a role for dysfunctional glutamate N-methyl-D-aspartate receptor (NMDAR) neurotransmission in schizophrenia. Accordingly, compounds that inhibit the glycine-1 transporter or target the glycine-binding site of NMDARs, including the co-agonists D-serine and glycine, have shown promise in treating the symptoms of schizophrenia. Together with D-serine, another D-form amino acid, D-Asp, exists in the brain of mammals. Synthesised by the enzyme aspartate racemase, D-Asp is highly concentrated in the prenatal brain; after birth, its levels sharply decrease due to the catabolising activity of the enzyme D-aspartate oxidase. D-Asp is able to stimulate NMDAR-dependent neurotransmission through direct action at the glutamate-binding site of NMDARs, thus functioning as an endogenous agonist for this subclass of glutamate receptors. The agonistic activity exerted by D-Asp on NMDARs and its neurodevelopmental occurrence make this D-amino acid a potential mediator for some of the NMDAR-related alterations observed in schizophrenia. Therefore, aim of the research is to investigate about the potential role of D-Asp in schizophrenia-relevant circuits and behaviors.

3. Results

3.1 D-aspartate levels in the *post-mortem* prefrontal cortex and caudate putamen of schizophrenia patients

As indicated above, an increasing number of evidence shows that D-Asp activates NMDAR-dependent transmission (Errico et al., 2008b; Errico et al., 2008a; Errico et al., 2011c; Errico et al., 2011b; Errico et al., 2011a), whose deregulation has been implicated in the pathophysiology of SCZ (Javitt, 1987; Goff and Coyle, 2001; Sawa and Snyder, 2003; Coyle, 2012; Javitt, 2012). Therefore, we measured the levels of D-Asp in two brain areas known to be involved in the pathophysiology of this illness, such as the prefrontal cortex and the *caudate putamen* (Tan et al., 2007; Howes and Kapur, 2009) of *post-mortem* SCZ patients. To this aim, we have used high-performance liquid chromatography (HPLC), based on the diastereomeric derivatization. In brief, amino acids contained in the biological matrix were derivatized to pairs of diastereomers with o-phthalaldehyde (OPA) and an optically active thiol reagent [N-acetyl-L-cysteine (NAC) that make them fluorescent. Then, the diastereomers were separated on non-chiral stationary phases, such as octadecylsilyl silica gel (ODS)-C18 column and finally detected fluorometrically at the proper wavelength. Interestingly, we have founded a consistent decrease of D-Asp levels both in the prefrontal cortex [Ctrl vs. SCZ (mean±SEM): 77.14±7.08 nmol/g tissue vs. 44.10±2.62 nmol/g tissue, 43% reduction, p=0.0002, one-way ANOVA; Fig. 3.1a] and *caudate putamen* [Ctrl vs. SCZ (mean±SEM): 104.14±12.59 nmol/g tissue vs. 61.80±4.30 nmol/g tissue, 41% reduction, p=0.002, one-way ANOVA; Fig. 3.1e] of SCZ patients compared with control individuals. Consistent with this strong reduction in D-Asp content, also the amount of its N-methyl derivative, NMDA, is reduced in the two brain areas of SCZ subjects analyzed [Ctrl *vs.* SCZ (mean ± SEM): prefrontal cortex, 5.26 ± 0.36 nmol/g tissue *vs.* 2.77 ± 0.18 nmol/g tissue, 47% reduction; caudate putamen, 9.79 ± 1.56 nmol/g tissue *vs.* 3.22 ± 0.34 nmol/g tissue, 67% reduction; $p <$ 0.01, per each brain area, Mann-Whitney test; Figure 3.1b and 3.1f]. Variation in D-Asp levels can depend on the change in the levels of its precursor, L-Asp. However, our analysis display comparable levels of this L-amino-acid between controls and SCZ individuals in both areas analysed [Ctrl vs SCZ (mean ± SEM): prefrontal cortex, 4.69

± 0.20 µmol/g tissue vs 4.25 ± 0.13 µmol/g tissue; caudate putamen, 5.22 ± 0.14 µmol/g tissue vs 4.82 ± 0.18 µmol/g tissue; $p > 0.05$, per each brain area, Mann-Whitney test; Figure 3.1c and g]. Finally, we examined the levels of the principal agonist of NMDARs, L-Glu. While L-Glu levels in the prefrontal cortex did not vary significantly between the two diagnostic groups [Ctrl vs SCZ (mean ± SEM): 8.75 ± 0.20 µmol/g tissue vs 8.63 ± 0.13 µmol/g tissue, $p > 0.05$, Mann-Whitney test; Figure 3.1d], in the caudate putamen we found a slight reduction of this amino acid in SCZ samples, compared to controls [Ctrl vs SCZ (mean ± SEM): 11.04 ± 0.47 µmol/g tissue vs 9.76 ± 0.25 µmol/g tissue, 12% reduction; $p < 0.05$, Mann-Whitney test; Figure 3.1h].

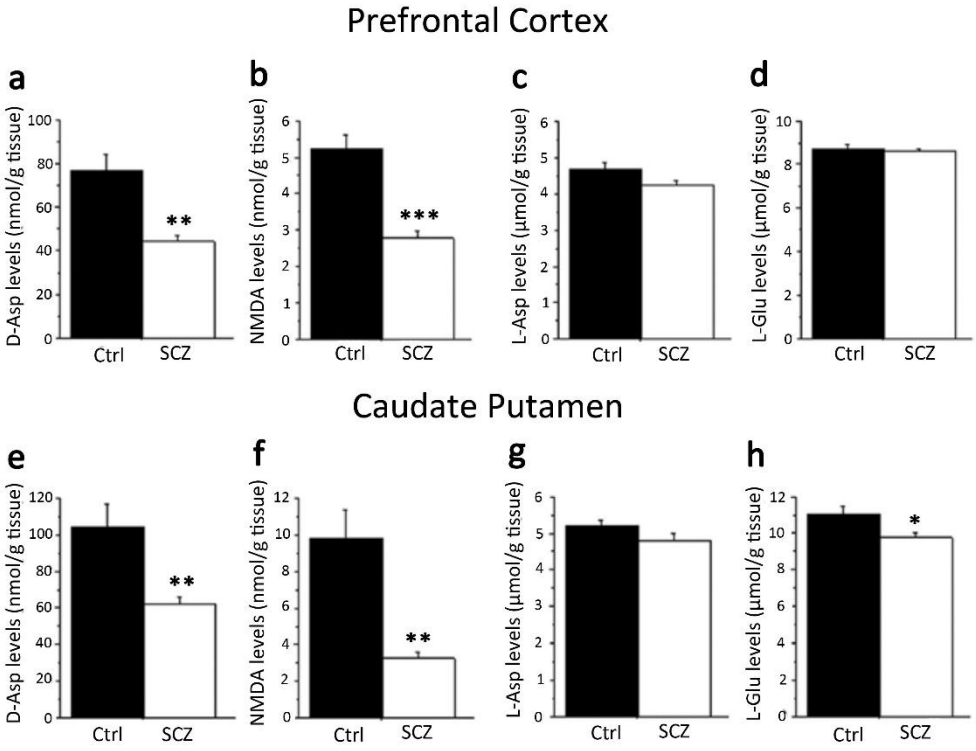

Figure 3.1: Detection of amino acids in the post-mortem brain samples of schizophrenia patients. The amino acids (**a, e**) D-aspartate (D-Asp), (**b, f**) N-methyl D-aspartate (NMDA), (**c, g**) L-aspartate (L-Asp) and (**d, h**) L-glutamate (L-Glu) were measured by HPLC in the prefrontal cortex (**a-d**) and *caudate putamen* (**e-h**) of control (Ctrl, n = 7) and schizophrenia subjects (SCZ, n = 10). * $p < 0.05$, ** $p < 0.01$, *** $p < 0.0001$, compared to control group (Mann-Whitney test). Values are expressed as mean ± SEM.

3.2 Expression of NMDAR subunits are selectively reduced in the *post-mortem* prefrontal cortex of schizophrenia patients.

In order to evaluate whether a constitutive deregulation of D-Asp levels may correlate with the expression of L-Glu receptors, we detected the levels of NMDAR subunits in the brain of SCZ patients. Interestingly, western blotting analysis displayed a significant decrease of GluN1 [p = 0.0100, Mann-Whitney test], GluN2A [p = 0.0238, Mann-Whitney test] and GluN2B [p = 0.0242, Mann-Whitney test] subunits in the prefrontal cortex of SCZ patients compared to controls (Figure 3.2 top panel). Conversely, in the caudate putamen the protein levels of each of the NMDAR subunits analyzed are comparable between SCZ and controls patients [p > 0.1, per each protein, Mann-Whitney test; Figure 3.2 bottom panel]. The present data is in line with the hypothesis of a reduced glutamatergic function in SCZ and, notably, with a substantial involvement of a cortical alteration of NMDAR-dependent neurotransmission.

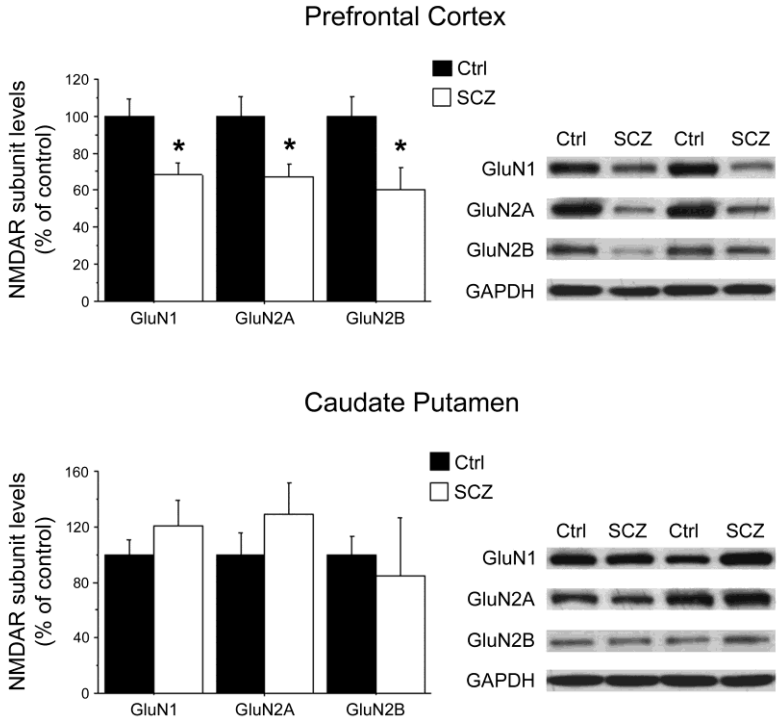

Figure 3.2: Expression of NMDAR subunits in the post-mortem brain samples of schizophrenia patients. Expression of the subunits GluN1, GluN2A and GluN2B of the NMDAR was evaluated by western blotting in the post-mortem prefrontal cortex and caudate putamen of control individuals (Ctrl) and schizophrenia patients (SCZ). GAPDH protein was used to normalize variations in loading and transfer. Representative blots comparing the two diagnostic groups are shown for each protein detected and brain region analyzed. * $p < 0.05$, compared to control group (Mann-Whitney test). Values are expressed as mean ± SEM.

3.3 DDO mRNA expression and methylation of the DDO gene in the post mortem SCZ brain

Variation in the mRNA content can depend on changes in the methylation degree within the regulatory regions of the corresponding gene. Therefore, we assessed whether the increase in *DDO* mRNA levels found in the PFC of SCZ patients could be associated with potential methylation changes in the CpG sites surrounding the ATG transcription start codon of the *DDO* gene. Our results showed that the pattern of methylation was unchanged in the PFC of patients, compared with control subjects [P>0.05 per each CpG site, analysis of covariance with covariance for post mortem delay, Figure 3.3b]. Therefore, the increase in *DDO* mRNA is not directly associated with methylation of the putative promoter region of the *DDO* gene.

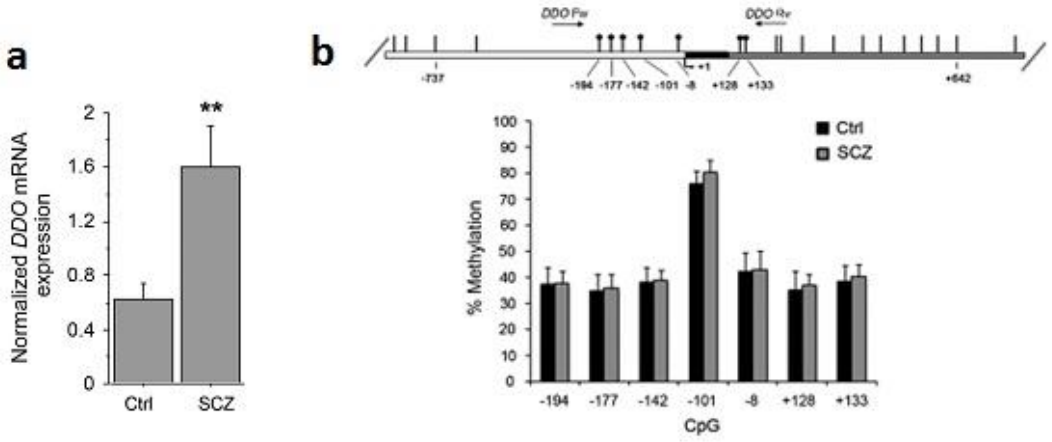

Figure 3.3: *DDO* mRNA expression and methylation of the *DDO* gene in the *postmortem* schizophrenia (SCZ) brain. (**a**) Analysis of *DDO* mRNA expression was performed by quantitative reverse transcription (qRT)-PCR in the PFC of SCZ patients and control individuals (Ctrl). Quantity means of transcript were normalized to the geometric mean of three housekeeping genes. (**b**) *DDO* gene methylation analysis by NGS. The top panel shows the structure of the putative promoter of human *DDO* gene. The transcriptional start site (+1) is indicated by an arrow. The putative regulatory upstream region (white box), exon (black) and first intron (striped box) are indicated. The primer positions used for methylation analysis are indicated by arrows (*DDO* Fw and *DDO* Rv). Vertical bars represent the relative positions of each CpG site. Black circles represent the CpG sites analyzed (CpG−194,−177,−142,−101,−8, +128 and +133). The bar graph below shows the methylation degree of single CpG sites at *DDO* promoter in the PFC of SCZ patients (gray bars) and Ctrl subjects (black bars) at each CpG site. **P<0.01, ANCOVA. All the values are expressed as mean±s.e.m.

3.4 LC/MSMS in *Ddo*$^{-/-}$

Results obtained in SCZ patients provide a stimulating hint for suggesting a potential role of D-Asp in the pathophysiology of this psychiatric illness. Therefore, we moved from human to mouse model with high levels of D-Asp (Errico et al., 2006; Errico et al., 2008a; Errico et al., 2011b) to evaluate the effect of deregulated levels of this molecule in NMDAR-dependent function and SCZ-like phenotype. For this purpose, we have developed a simple and rapid method for the simultaneous direct measurement of D-Asp, L-Asp and NMDA in brain tissue based on chiral fractionation of enantiamers and tandem mass spectrometry in multiple reaction monitoring (MRM) mode avoiding any derivatization step and with greater sensitivity than HPLC previously used. The MRM method allowed us to discriminate the target metabolites within the very complex mixture originated from tissue extracts. Briefly, D-Asp, L-Asp and NMDA were directly resolved by HPLC on a Chirobiotic chiral stationary phases consisting of the amphoteric glycopeptide Teicoplanin covalently bound to silica gel and all three compounds could be unambiguously identified by their specific MRM transitions. All the analytical parameters, LOD, LOQ and LLOQ were determined. In Figure 3.4 are showed representative chromatogram obtained in our detection. In the first two panel are represented the chromatograms of standard solution of L-Asp (Figure 3.4a) or a mixture of L and D-Asp (Figure 3.4b), in order to evaluate the retention time of this amino acids and to confirm that this method is able to discriminate D- and L-form. Moreover, several tests were performed using mouse brain tissues as source of metabolites to evaluate the performances of the procedure in the presence of the matrix (Figure 3.4c). First, the concentration of L-Asp was determined in adult mouse brain samples showing clear detection of the metabolite and the complete absence of D-Asp, as expected. Neither interferences nor carryover peaks were observed in the MRM analysis. Then, different amounts of D-Asp (Figure 3.4d), L-Asp or NMDA were spiked in mouse brain extracts and the recovery of the target metabolites was estimated always displaying values better than 90% for each analyte.

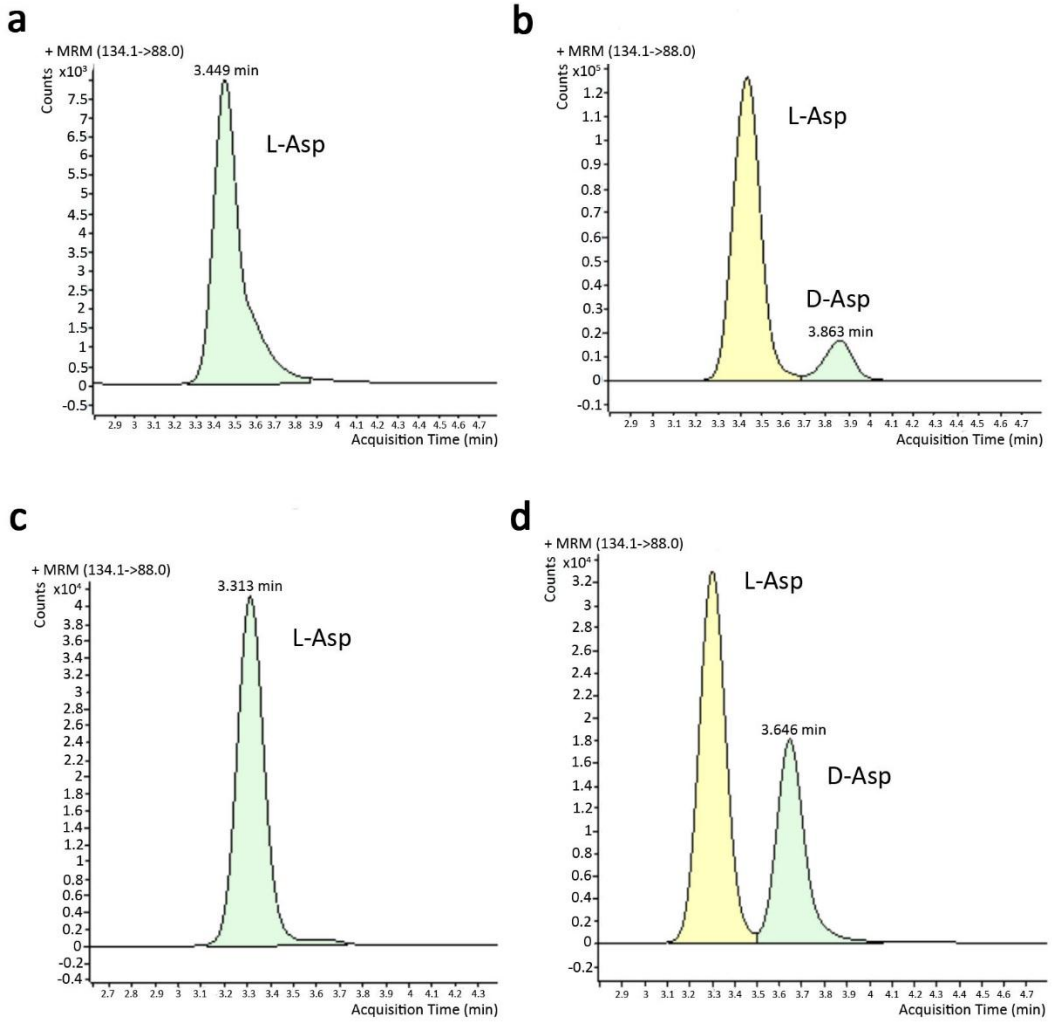

Figure 3.4: Representative LC-MS/MS chromatograms. (**a**) standard L-Asp solutions; (**b**) standard mixture of D- and L-Asp; (**c**) mouse brain extract; (**d**) mouse brain extract + spike of D-Asp.

Finally, the developed procedure was applied to the quantitative determination of D-Asp and L-Asp in many brain samples from mouse models, and the results were compared with the same measurements carried out by HPLC. For the measurements we used mice with target deletion of Ddo gene (named *Ddo* knockout, $Ddo^{-/-}$) and their relative controls (named *Ddo* wild type, $Ddo^{+/+}$). Comparing HPLC and LC-MS/MS in MRM results, we showed that the absolute amount of D-Asp levels were different [HPLC: $Ddo^{-/-}$ 1384,446 nmol/g; $Ddo^{+/+}$ 45,048 nmol/g; LC-MS/MS: $Ddo^{-/-}$ 5148,443 nmol/g ; $Ddo^{+/+}$ 259,420 nmol/g], but D/L ratio is approximately the same [HPLC: $Ddo^{-/-}$ 0,624; $Ddo^{+/+}$ 0,019; LC-MS/MS: $Ddo^{-/-}$ 0,441; $Ddo^{+/+}$ 0,012] (Figure 3.5).

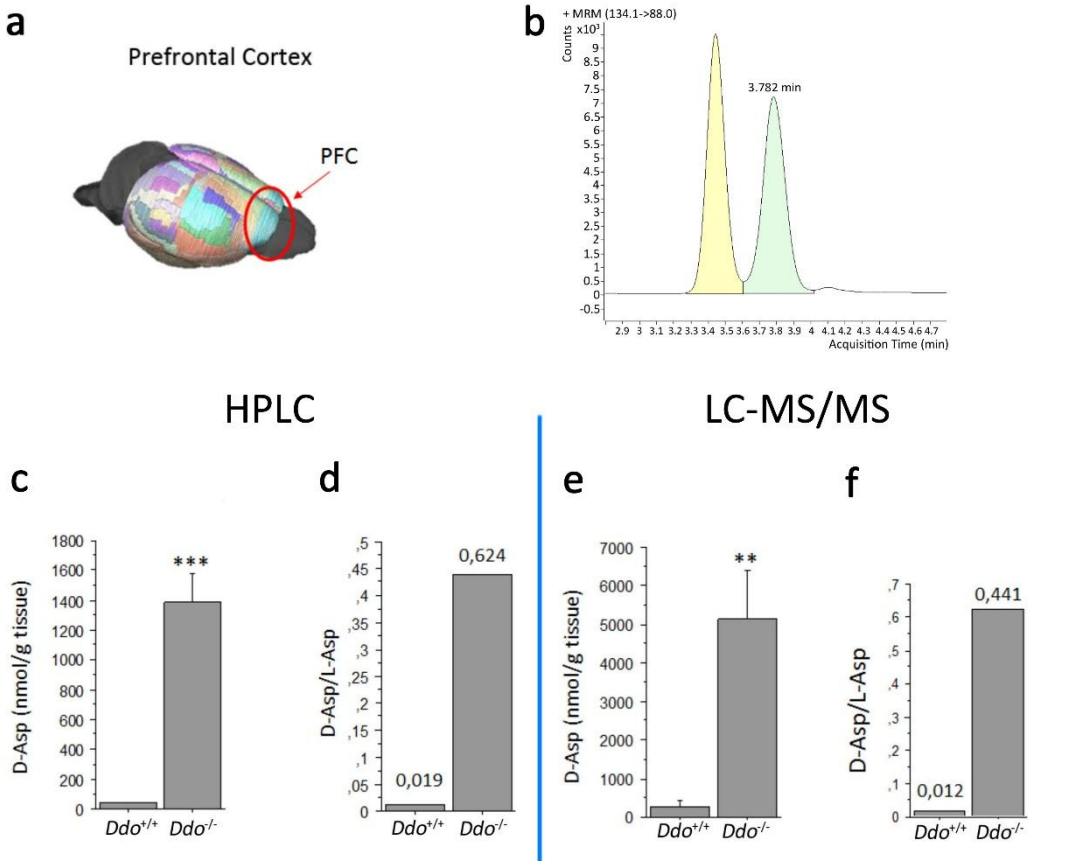

Figure 3.5: D-Asp detection in the PFC: comparison between HPLC and LC-MS/MS. (**a**) schematic representation of PFC; (**b**) representative LC-MS/MS chromatogram of D- and L-Asp detection in *Ddo*$^{-/-}$ PFC (**c,e**) D-Asp detection and (**d,f**) D/L ratio in the PFC obtained by (**c,d**) HPLC; (**e,f**) LC-MS/MS.

Notably, we confirmed that target deletion of Ddo gene results in increased levels of D-Asp in different mouse brain area [PFC: p=0,0038; Hippocampus: p=0,0376; Cerebellum: p=0,0003, Student t test] (Fig. 3.5 and 3.6), while no difference was found in L-Asp content [p>0,05 in all brain area; Student t test] (Fig.3.6).

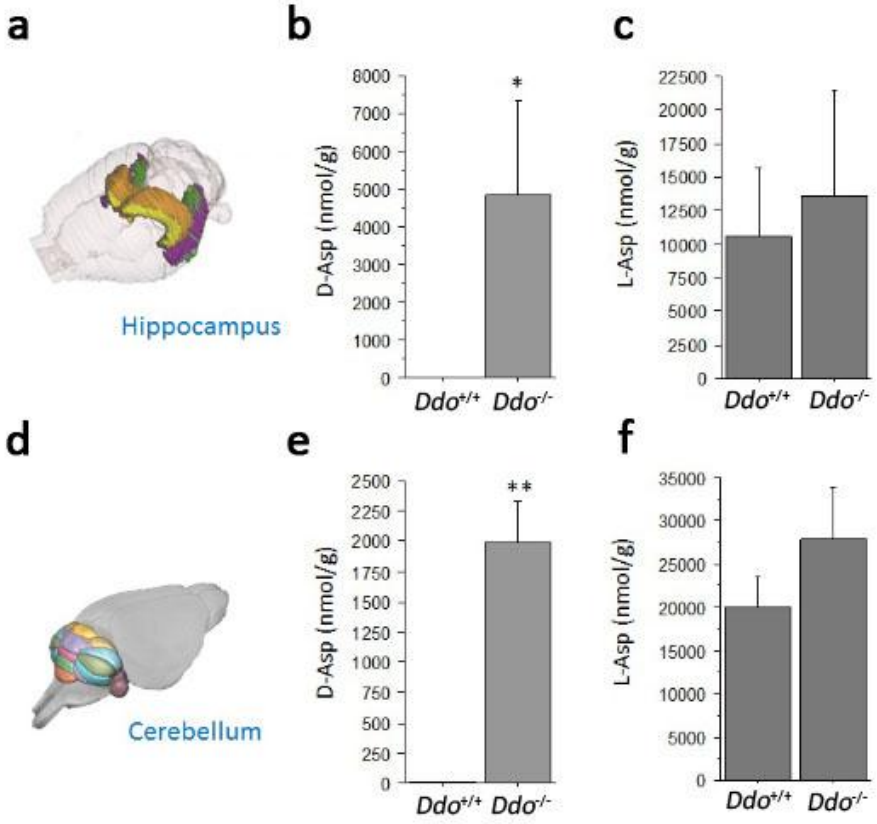

Figure 3.6: LC-MS/MS detection in the hippocampus and cerebellum of *Ddo*$^{+/+}$ and *Ddo*$^{-/-}$ mice. (**a**) schematic representation of mouse hippocampus; (**b**) D-Asp and (**c**) L-Asp detection in the hippocampus; (**d**) Graphic display of cerebellum (**e**) D-Asp and (**f**) L-Asp levels in the cerebellum.

The simultaneous, sensitive, fast, and reproducible measurement of these metabolites enabled us to correlate the amount of D-Asp with relevant pathophysiological processes.

3.5 Dendritic morphology in mice with high levels of D-Aspartate

Dendrite morphogenesis is a complex but well-orchestrated process and includes the development of dendritic branches, forming characteristic dendrite arbors, and dendritic spines, allowing neurons to communicate with each other. Emerging evidence reveals that dendritic spine and dendrite arbor stability have crucial roles in the correct functioning of the adult brain and that loss of stability is associated with psychiatric disorders and neurodegenerative diseases (Kulkarni and Firestein, 2012).

Particularly, reductions in dendritic arbor size and spine number have been reported in individuals with schizophrenia (Glantz and Lewis, 2000).

NMDA receptor signaling appears to have a major role in dendritic growth and the formation of new synapses (Lamprecht and LeDoux, 2004; Collingridge et al., 2013). Therefore, considering the ability of D-Asp to activate this type of Glu receptor, we investigated the effect of increased levels of D-Asp on neuronal morphology by Golgi-Cox analysis. After 1-month-chronic treatment with D-Asp, pyramidal neurons of the PFC exhibited significantly increased dendritic length, compared with untreated animals [H_2O vs D-Asp (mean ± s.e.m.): 1564.33 ± 62.16μm vs 2068.94 ± 49.13μm,$P<0.01$; Figure 3.7a]. This morphological phenotype is also accompanied by greater complexity of dendritic tree between 25 and 125μm in basal dendritic segments [$P<0.01$ at 25, 50, 75 and 100μm; $P<0.05$ at 125μm] and 200 and 250μm in apical dendritic segments [$P<0.05$] (Figure 3.7b). Moreover, in this region we found increased spine density in D-Asp treated mice compared to controls [H_2O vs D-Asp (mean ± s.e.m.): 3.03 ± 0.25 spines per 10μm vs 4.01 ± 0.25 spines per 10μm,$P<0.05$; Figure 3.7c].

Next, we examined dendritic architecture of pyramidal neurons in the CA1 area of the hippocampus of D-Asp-treated mice. As in the PFC, also in this brain region we found a significant extension in the length of the dendrites [H_2O vs D-Asp (mean ± s.e.m.): 1925.80 ± 98.97μm vs 2352.93 ± 126.97μm, $P<0.05$; Figure 3.7d] and increased spine density [H_2O vs D-Asp (mean ± s.e.m.): 4.74 ± 0.25 spines per 10μm vs 5.78 ± 0.33 spines per 10μm,$P<0.05$; Figure 3.7f] in treated animals, compared with controls (Figure 3.7e).

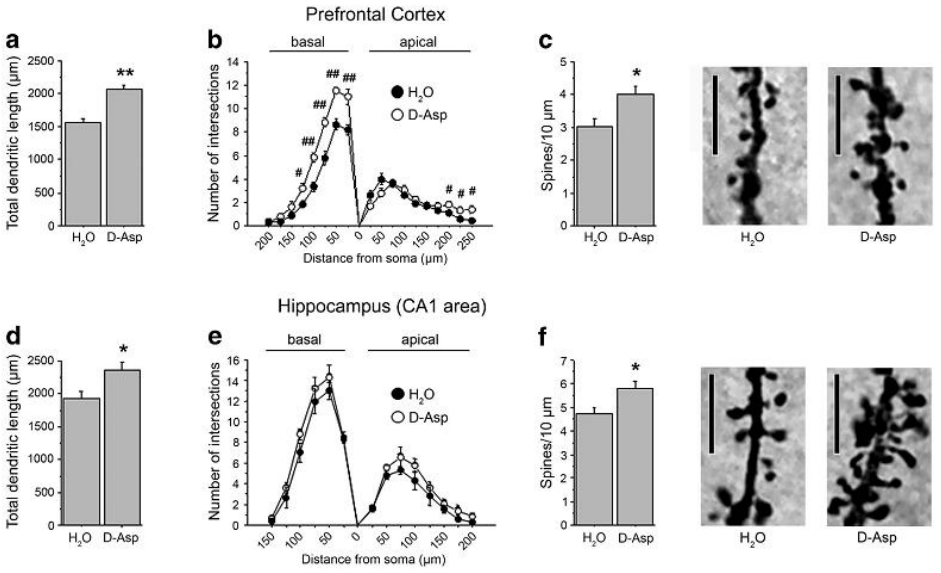

Figure 3.7: Analysis of dendritic morphology was performed on C57BL/6J mice drinking D-Asp or H_2O in pyramidal neurons of the (**a–c**) PFC and (**d–f**) CA1subfield of the hippocampus after Golgi-Cox staining. (**a** and **d**) Total dendritic length (in µm) measured in the (**a**) PFC and (**d**) CA1 subfield of the hippocampus. (**b** and **e**) Number of intersections between basal or apical dendrites and Sholl concentric circle lines at different distances from soma center in both (**b**) PFC and (**e**) CA1 area. Concentric circles increase in diameter by 25µm increments. (**c** and **f**) Spine density (number of spines per 10µm) evaluated in (**c**) the PFC and (**f**) CA1 area of mice. The right panels show representative dendrites. **P<0.01, *P<0.05, compared with untreated mice (Student'st-test). ##P<0.01, #P<0.05, compared with untreated mice (Fisher'spost hoc). Scale bar, 5µm.

To confirm the capability of D-Asp to influence the neuronal morphology, we also used knockout mice for *Ddo* gene. Similar to chronic treatment with D-Asp, we found increased total dendritic length in $Ddo^{-/-}$ mice compared to control littermates both in the PFC [$Ddo^{+/+}$ vs $Ddo^{-/-}$ (mean ± s.e.m.): 1189.37 ± 28.63µm vs 1537.47 ± 138.10µm,P<0.05; Figure 3.8a] and CA1 area of the hippocampus [$Ddo^{+/+}$ vs $Ddo^{-/-}$ (mean ± s.e.m.): 1765.25 ± 117.58µm vs 2219.51 ± 43.86µm,P<0.01; Figure 3.8d]. Sholl analysis revealed no difference in the complexity of basal and apical dendrites in the PFC (Figure 3.8b). On the other hand, in the CA1 area we found a greater number of intersections in the basal dendrites of $Ddo^{-/-}$ mice between 50 and 125µm, compared with controls [P<0.01 at 50µm;P<0.05 at 75, 100 and 125µm, Figure 3.8e]. At last, dendrites from $Ddo^{-/-}$ neurons have greater spine density compared with control neurons in both areas analyzed [PFC: $Ddo^{+/+}$ vs $Ddo^{-/-}$ (mean ± s.e.m.): 2.12 ± 0.09 spines per 10µmvs 2.76 ± 0.24 spines per 10µm,P<0.05; Figure 3.8c; Hippocampus: $Ddo^{+/+}$ vs $Ddo^{-/-}$ (mean ± s.e.m.): 3.99 ± 0.16 spines per 10µm vs 4.53 ± 0.13 spines per 10µm, P<0.05; Figure 3.8f].

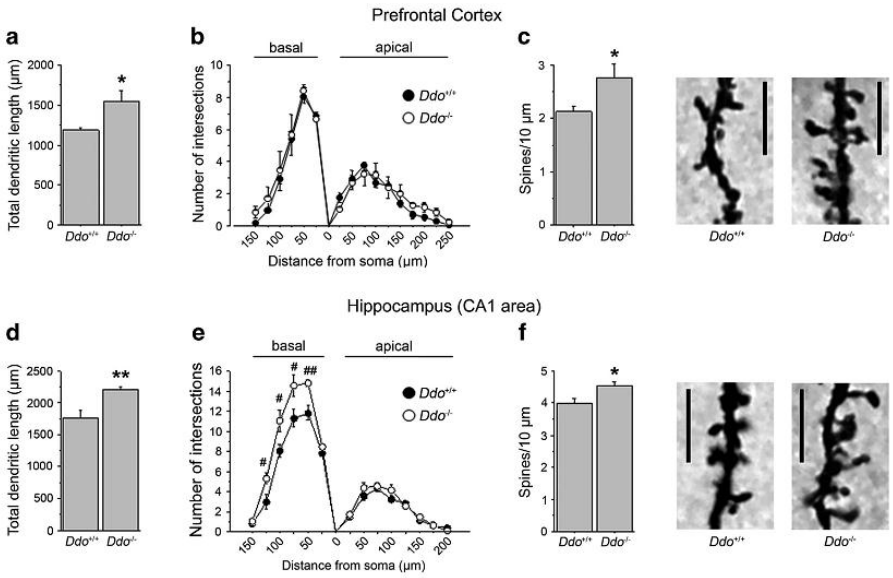

Figure 3.8: Analysis of dendritic morphology was performed on *Ddo*$^{+/+}$ and *Ddo*$^{-/-}$ mice in pyramidal neurons of the (**a–c**) PFC and (**d–f**) CA1subfield of the hippocampus after Golgi-Cox staining. (**a** and **d**) Total dendritic length (in µm) measured in the (**a**) PFC and (**d**) CA1 subfield of the hippocampus. (**b** and **e**) Number of intersections between basal or apical dendrites and Sholl concentric circle lines at different distances from soma center in both (**b**) PFC and (**e**) CA1 area. Concentric circles increase in diameter by 25µm increments. (**c** and **f**) Spine density (number of spines per 10µm) evaluated in (**c**) the PFC and (**f**) CA1 area of mice. The right panels show representative dendrites. **P<0.01, *P<0.05, compared with *Ddo*$^{+/+}$ mice (Student'st-test). ##P<0.01, #P<0.05, compared with *Ddo*$^{+/+}$ mice (Fisher'spost hoc). Scale bar, 5µm.

3.6 High levels of D-Asp converts E-LTP into L-LTP in the adult hippocampus

Dendritic spine density is strictly correlated with functional synaptic plasticity (Matsuzaki et al., 2004; Okamoto et al., 2004), in particular with long-lasting forms of synaptic potentiation, in which NMDARs are known to play a major role (ref). Given the ability of D-Asp to induce dendritic structural modifications and enhance early-phase LTP (refs), we evaluated whether this D-amino acid was also able to affect late-phase synaptic plasticity in the mouse hippocampus. As expected, using an early-phase LTP (E-LTP) induction paradigm (100 Hz, 1 s), we observed a decaying LTP in mice drinking water and in wild-type slices after 1 h. Strikingly, this protocol was sufficient to induce stablelate-phase (L-LTP) both in D-Asp-treated [LTP at 160 min, H_2O = 16 ± 7%; D-Asp = 57 ± 7%;*t*-test, last 10 min of recording, P<0.001; Figure 3.9a] and *Ddo*$^{-/-}$ mice [LTP at 160 min, *Ddo*$^{+/+}$ = 14 ± 5%, *Ddo*$^{-/-}$ = 36 ± 5%; t-test, last 10 min

of recording, P<0.001; Figure 3.9d]. To investigate the nature of lowered threshold for the induction of L-LTP in presence of higher levels of D-Asp, we administered rapamycin before the conditioning train. In fact it is known that long lasting form of LTP is sensitive to this compounds (Tang et al., 2002; Costa-Mattioli et al., 2009). Notably, also in this condition L-LTP still persisted in both mouse models [*D-Asp treated*: LTP at 160 min, vehicle = 57 ± 7%, rapamycin = 53 ± 4%; t-test, last 10 min of recording,P>0.05; Figure 3.9b; *Ddo*$^{-/-}$: LTP at 160 min, vehicle = 36 ± 5%, rapamycin = 28 ± 5%; t-test, last 10 min of recording, P>0.05; Figure 3.9e]. It has been demonstrated that cytoskeletal stability is crucial for maintaining long-lasting forms of LTP (Huang et al., 2013). Interestingly, treatment with cytochalasin D, an actin polymerization inhibitor, fully prevented L-LTP in D-Asp treated [LTP at 160 min, vehicle = 57 ± 7%, cytochalasin D = 4 ± 5%;t-test, last 10 min of recording, P<0.001; Figure 3.9c] and *Ddo*$^{-/-}$ mice [LTP at 160 min, vehicle = 36 ± 5%, cytochalasin D = 5 ± 8%;t-test, last 10 min of recording, P<0.001; Figure 3.9f].

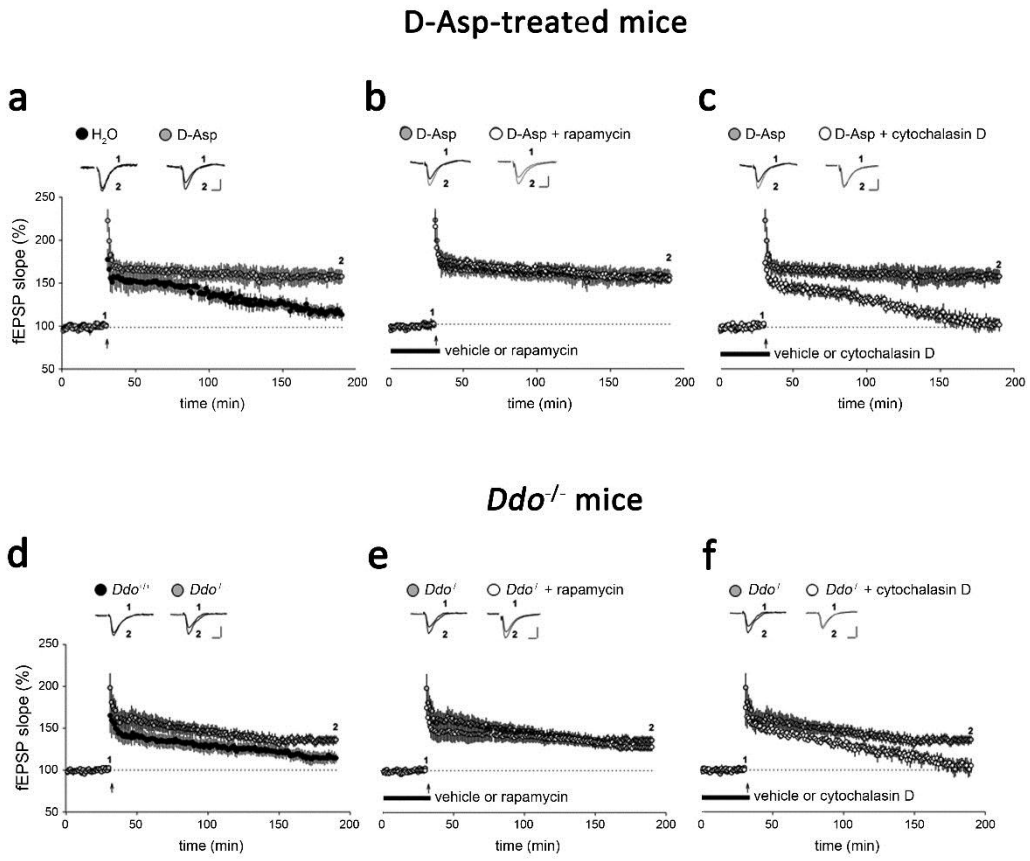

Figure 3.9: Late-phase LTP in D-Asp-treated and *Ddo*$^{-/-}$ mice. Time plot of hippocampal fEPSP responses showing the effect of E-LTP stimulation paradigm in (**a**) untreated C57BL/6J mice and D-Asp-treated C57BL/6J mice and (**d**) *Ddo*$^{+/+}$ and *Ddo*$^{-/-}$ mice . Hippocampal L-LTP in (**b**) D-Asp-treated and (**e**) *Ddo*$^{-/-}$ mice was unaffected following bath-application of 20 nM rapamycin (transiently bath-applied for 40 min) but was fully blocked following bath-application of 100 nM cytochalasin D (continuously bath-applied) as showed in the panels (**c**) and (**f**). Insets show field EPSPs from representative experiments during baseline and following LTP induction (1 s, 100 Hz tetanus). Vertical bar, 0.5 mV; horizontal bar, 10 ms.

3.7 Increased levels of D-Asp affect schizophrenia-like behavior induced by PCP in mice.

We then evaluated the effect of deregulated high levels of D-Asp on SCZ-like behaviors. To this aim we challenged *Ddo*$^{-/-}$ animals with phencyclidine (PCP). This drug mirrors the symptomatology of SCZ in humans (Domino, 1964; Allen and Young, 1978), primates and rodents (Morris et al., 2005; Jones et al., 2011; Javitt et al., 2012; Moghaddam and Krystal, 2012) by blocking NMDARs. First, we evaluated PCP-induced hyper-locomotion at two different doses, 3 and 6 mg/kg (Figure 3.10).

As expected, this drug caused increasing motor hyperactivity in *Ddo*$^{+/+}$ mice at the two doses analyzed (Figure 3.10). In *Ddo*$^{-/-}$ mice, 3 mg/kg PCP produced locomotor stimulation similar to that evoked in *Ddo*$^{+/+}$ animals [three-way ANOVA with repeated measures: treatment × genotype, $F_{(1,240)} = 0.173$, P= 0.6789]. Interestingly, at the dose of 6 mg/kg, *Ddo*$^{-/-}$ animals show attenuated motor hyperactivity compared to wild-type littermates [two-way ANOVA with repeated measures: genotype effect, $F_{(1,120)} = 6.952$,P= 0.0145] (Figure 3.10).

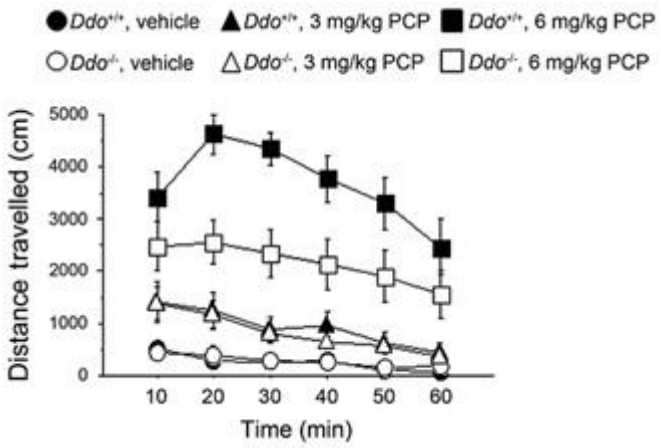

Figure 3.10: Motor activity induced by 3 mg/kg or 6 mg/kg PCP in *Ddo*$^{+/+}$ and *Ddo*$^{-/-}$ mice. Locomotion was expressed as distance traveled, measured in cm every 10 min over a 60-min session and presented as time course.

Next, using a Prepulse Inhibition (PPI) paradigm, we investigate the effect of PCP on sensorimotor gating of *Ddo*$^{-/-}$ mice (figure 3.11). PPI is a paradigm commonly used to evaluate SCZ-like symptoms both in animal models and in humans. This test evaluates the integrity of sensorimotor gating, a function often destroyed in SCZ patients. As expected, PCP at the dose of 3 mg/kg significantly destroyed PPI in *Ddo*$^{+/+}$ animals [two-way ANOVA with repeated measures: treatment effect, $F_{(1,54)} = 4.906$, P= 0.0399; Figure 3.11a]. Conversely, in *Ddo*$^{-/-}$ 3mg/kg PCP does not produce any effect on sensorimotor gating, as revealed by a comparable startle amplitude between treated and vehicle-treated mice [$F_{(1,54)}$= 1.668, P= 0.2129; Figure 3.11a]. Conversely, the dose of 6 mg/kg PCP caused PPI deficits in both *Ddo*$^{+/+}$ and *Ddo*$^{-/-}$ mice [treatment effect: *Ddo*$^{+/+}$, $F_{(1,54)} = 6.919$, P= 0.0170; *Ddo*$^{-/-}$, $F_{(1,54)} = 6.343$,P= 0.0215; Figure 3.11b].

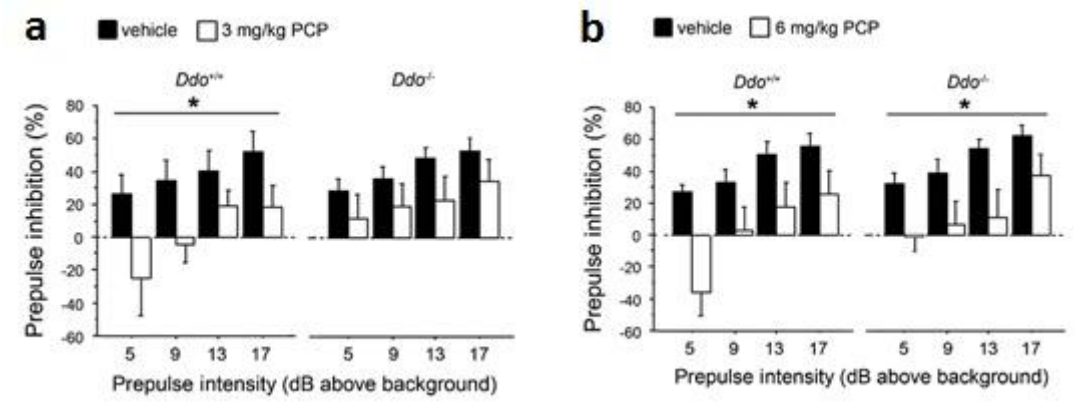

Figure 3.11: PPI deficits induced by (**a**) 3 mg/kg or (**b**) 6 mg/kg PCP in *Ddo*$^{+/+}$ and *Ddo*$^{-/-}$ mice. Percentage of the PPI was used as dependent variable and measured at different prepulse intensities (dB above 65 dB background level). *P<0.05, compared with vehicle control groups. All the values are expressed as the mean±s.e.m.

Taken together, these results point to a reduced reactivity to PCP-induced psychotomimetic behaviors in *Ddo*$^{-/-}$ animals, compared to wild-type littermates.

To evaluate whether increased D-Asp levels are always able to protect against sensorimotor deficits produced by PCP or, rather, it is important the time-window in which D-Asp content increases, we repeated PPI experiments in C57BL/6 mice chronically treated with D-Asp for 1 month (20 mM in tap water), during adulthood. At the dose of 3 mg/kg, pretreatment with D-Asp did not significantly alter the PPI deficits induced by PCP [D-Asp pretreatment effect: $F_{(1,99)}$= 2.386, P= 0.1320; D-Asp pretreatment × PCP treatment: $F_{(1,99)}$= 0.026, P= 0.8726; Figure 3.12a]. We found similar results after 6 mg/kg PCP treatment [D-Asp pretreatment effect: $F_{(1,102)}$= 0.732, P= 0.3983;D-Asp pretreatment × PCP treatment: $F_{(1,102)}$ = 0.017, P= 0.8960; Figure 3.12b].

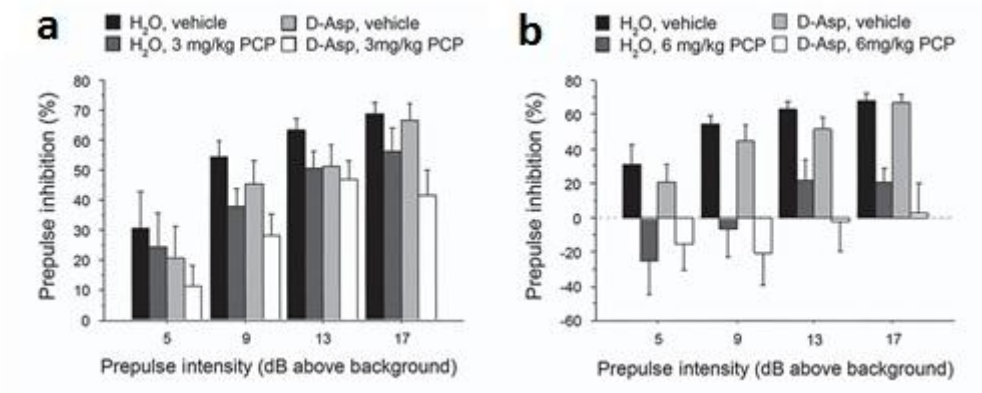

Figure 3.12: Prepulse inhibition responses to PCP after 1-month oral administration of D-Asp in mice treated with (**a**) 3 mg/kg PCP or vehicle, (**b**) 6 mg/kg PCP or vehicle. Percentage of the PPI was used as dependent variable and measured at different prepulse intensities (shown as dB above 65 dB background level). All the values are expressed as the mean±s.e.m.

3.8 fMRI response induced by PCP

Considering the ability of D-Asp to influence NMDAR activity and PCP-induced behaviors, we evaluated if increased levels of this D-amino acid can modulate the aberrant neuro-functional cascade underlying the psychotomimetic effect of PCP. To this purpose, we used fMRI to map the neural substrates recruited by a subanesthetic dose of PCP (intravenous, 1 mg/kg). Consistent with rodent and human imaging studies (Gozzi et al., 2008b; Bifone and Gozzi, 2012; De Simoni et al., 2013; Doyle et al., 2013), control mice showed a robust cortico–limbo–thalamic fMRI response to the drug, with a prominent involvement of the prefrontal–orbitofrontal, cingulate and visual cortex, ventral hippocampus and mediodorsal thalamic nuclei (Figures 3.13a). By contrast, a generalized attenuation of PCP-induced fMRI response was observed in *Ddo*$^{-/-}$ mice, with respect to wild-type animals (Figures 3.13b). Quantification of the effect in representative volume of interest revealed a statistically significant attenuation in several brain regions, including prefrontal, orbitofrontal anterior and posterior (retrosplenial) cingulate, visual and parietal cortex and ventral hippocampus [P>0.05 in all regions, Student'st-test; Figure 3.13c,d]. Overall, these results suggest that a challenge with PCP in *Ddo*$^{-/-}$ animals is associated with consistent alterations of blood flow in brain areas known to be involved in the pathophysiology of SCZ.

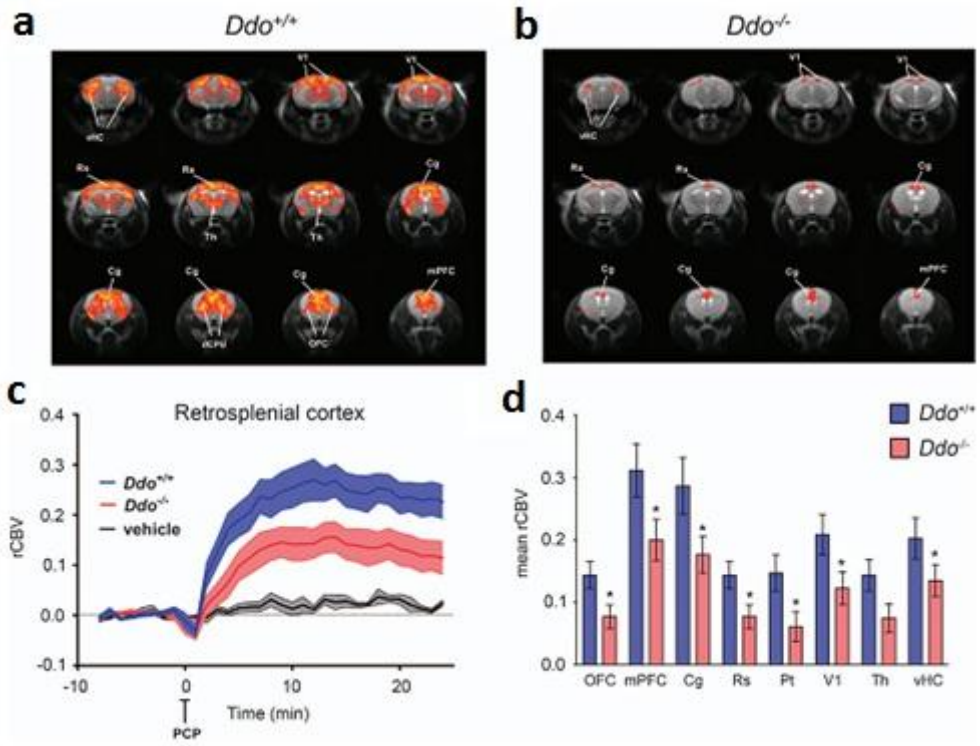

Figure 3.13: PCP-induced fMRI response in *Ddo*$^{-/-}$ mice. (**a** and **c**) In *Ddo*$^{+/+}$ mice, PCP elicited robust and sustained cortico–limbo–thalamic fMRI activation. (**b–d**) This effect was strongly attenuated in *Ddo*$^{-/-}$ mice. Red/yellow in **a** and **b** indicates significant fMRI (rCBV) response to PCP (1 mg/kg, intra-artery) with respect to vehicle (saline; 3.1<z-score<6, cluster correction threshold pc=0.001). *P<0.05, Student'st-test. Cg, cingulate cortex; dCPU, dorsal caudate putamen; fMRI, functional magnetic resonance imaging; mPFC, medial prefrontal cortex; OFC, orbitofrontal cortex; PCP, phencyclidine; rCBV, relative cerebral blood volume; Rs, retrosplenial cortex; Th, thalamus; vHc, ventral hippocampus; V1, visual cortex.

As in the case of PPI experiments, we then assessed the fMRI response induced by PCP after 1-month chronic D-Asp administration. Both D-Asp- and H_2O-treated mice exhibited a robust cortico–limbo–thalamic fMRI response to the drug, with a prominent involvement of the prefrontal–orbitofrontal, cingulate and visual cortex, ventral hippocampus and mediodorsal thalamic nuclei (Figures 3.14). However, no statistically significant inter-group difference in the response to PCP was observed either at the voxel level [z>1.6, cluster corrected at P<0.01) or when integrated at the level of volumes of interest (right panel; P>0.27, all regions, Student's t-test]. Overall, in contrast to *Ddo*$^{-/-}$ mice, D-Asp supplementation failed to produce any significant modulation of PCP-induced PPI and fMRI responses. The lack of inhibitory effect observed suggests that D-Asp elevation in normally developed brains may not be sufficient to prevent SCZ-like hyperglutamatergic state, and points at a putative neurodevelopmental origin for some of the phenotypes observed in *Ddo*$^{-/-}$ mice.

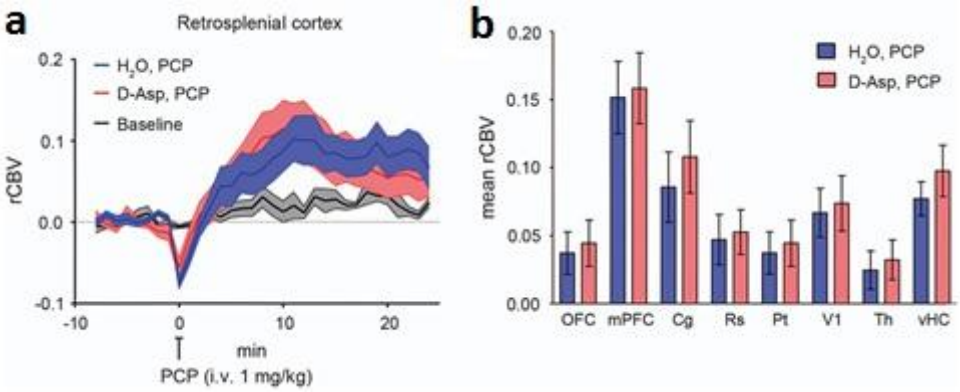

Figure 3.14: PCP-induced fMRI response in D-Asp- and H_2O-treated adult C57BL6/J mice. In both groups of animals, PCP elicited robust and sustained cortico–limbo–thalamic fMRI activation (**a** and **b** panels). No statistically significant difference in the inter-group response to PCP was observed either at the voxel level (z>1.6, cluster corrected at P<0.01) or when integrated at the level of volumes of interest (panel **b**; P>0.27, all regions, Student'st-test). Cg, cingulate cortex; dCPU, dorsal caudate putamen; fMRI, functional magnetic resonance imaging; mPFC, medial prefrontal cortex; OFC, orbitofrontal cortex; PCP, phencyclidine; rCBV, relative cerebral blood volume; Rs, retrosplenial cortex; Th, thalamus; vHc, ventral hippocampus; V1, visual cortex.

3.9 Does D-Asp cross the blood brain barrier?

In the light of the ability of exogenous D-Asp to influence NMDAR-mediated processes in the mouse brain, we investigated whether D-Asp can cross the blood brain barrier, a highly selective permeability barrier that separates the circulating blood from the brain extracellular fluid in the central nervous system. To this aim, we performed *in vivo* microdialysis experiments in the PFC of freely moving C57BL/6 mice treated with acute injection of 500 mg/kg D-Asp. Samples collected were analyzed for D-Asp and L-Asp content. Remarkably, this treatment caused a strong increase in extracellular D-Asp levels [two-way ANOVA with repeated measures, $F_{(1,80)}$ = 287.840; P<0.0001, Figure 3.15a] with a peak 40 min after injection [2430±170 nM, ~240-fold increase over basal levels, Figure 3.15a]. Moreover, D-Asp administration also affected free L-Asp content [$F_{(1,80)}$=8.011; P=0.0221; Fig. 3.15b], although the increase was smaller than that observed for D-Asp [230±10 nM, ~3-fold increase], and returned to baseline already 80 min after injection (Figure 3.15b). We also executed Analysis on PFC omogenates 2 h after D-Asp injection to evaluate if the changes in the extracellular levels of these amino acids mirror the total amount of these molecules. Results showed a strong increase of D-Asp in the PFC omogenate of D-Asp-treated

mice compared to vehicle-treated group [P=0.0289; Fig 3.15c], while no difference was found in L-Asp content [P=0.6809; Fig 3.15d].

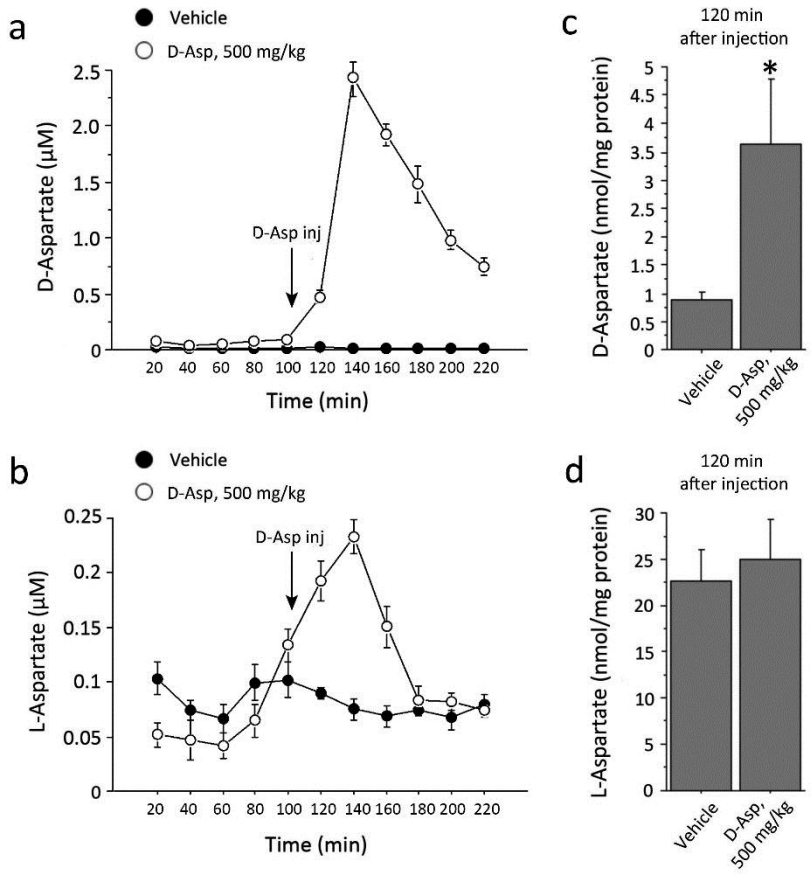

Figure 3.15: D-Asp and L-Asp extracellular concentration after acute administration of the D-Asp. (**a, b**) Time course of cortical extracellular concentration of free D-Asp and free L-Asp in control animals and in mice subjected to the acute i.p. administration of 500 mg/kg D-Asp. (**c, d**) Free D-Asp and free L-Asp total contents in PFC homogenates of control and acutely treated mice after 2 hours from treatment. The amount of D-Asp and L-Asp in tissue homogenates was normalized by the total protein content of each sample. The graphs displayed the mean values ± SEM; * $P < 0.01$ two-way ANOVA with repeated measures followed by Fisher's post hoc test for microdialysis analyses and Student's t test for homogenates analyses.

3.10 D-Asp is released in a calcium-dependent manner

We then performed in vivo microdialysis also on C57BL/6 mice treated for 1 month with D-Asp to measure the concentration of this D-amino acid in the dialysates collected from the PFC. As shown in Figure 3.16a, D-Asp extracellular levels were significantly increased by the treatment, at each time point analyzed [two-way ANOVA with repeated measures $F_{(1,32)}=11.045$, P=0.0105]. On the other hand, no

variation in the levels of the L-enantiomer was found between groups [two-way ANOVA with repeated measures $F_{(1,32)}$=0.614, P=0.4558; Figure 3.16b]. Interestingly, by removing calcium from the ACSF in the last dialysate fraction, we observed that free D-Asp levels, as well as free L-Asp, became undetectable (Figure 3.16a,b), thus proving that the release of this amino acid is Ca^{2+}-dependent. As reported after acute treatment, also in chronically treated mice we found a significant increase in D-Asp levels in the PFC homogenates, compared to controls [D-Asp vs. H_2O: 2.76±0.27 nmol/mg prot vs. 1.20±0.26 nmol/mg prot; P=0.0057, Student's t-test; Figure3.16c]. Conversely, the amount of L-Asp did not change with the treatment [D-Asp vs. H_2O: 29.4±1.5 nmol/mg prot vs. 30.7±1.5 nmol/mg prot; P=0.5759; Figure 3.16d).

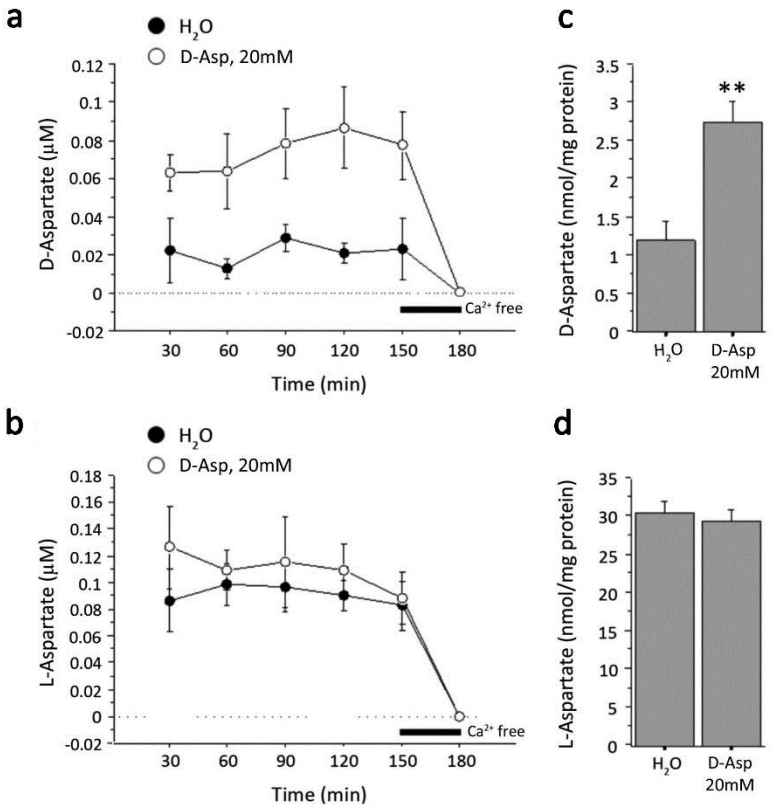

Figure 3.16: D-Asp release in the PFC of freely moving mice. (**a, b**) Cortical extracellular concentration of free D-Asp and free L-Asp in control animals and in mice subjected to the chronic administration of 20 mM D-Asp. (**c, d**) Free D-Asp and free L-Asp total contents in PFC homogenates of control and chronically treated mice. The amount of D-Asp and L-Asp in tissue homogenates was normalized by the total protein content of each sample. The graphs displayed the mean values±SEM; ** P<0.005 two-way ANOVA with repeated measures followed by Fisher's post hoc test for microdialysis analyses and Student's t-test for homogenates analyses.

3.11 D-Asp modulates L-Glutamate release in the mouse brain

We have previously described the ability of D-Asp to modulate NMDAR-dependent functions. Here, we investigated the consequences of elevated D-Asp content on the basal extracellular levels of L-Glu, the principal endogenous agonist of NMDARs. Interestingly, *in vivo* microdialysis performed in the hippocampus of adult *Ddo*$^{-/-}$ mice revealed an increase in L-Glu content, compared to *Ddo*$^{+/+}$ counterpart [two-way ANOVA with repeated measures $F_{(1,12)}$=14.87; P<0.01; Figure 3.17a]. The same analysis was carried out in the PFC of C57BL/6 mice treated with acute or chronic administration of D-Asp. Consistently, we observed a D-Asp-induced increase of L-Glu efflux both in acutely [two-way ANOVA with repeated measures $F_{(1,40)}$=25.578, P=0.001; Figure 3.17b] and chronically treated animals [two-way ANOVA with repeated measures $F_{(1,32)}$=34.454, P=0.0004; Fig. 3.17c], thus suggesting that D-Asp is able to produce the *in vivo* release of L-Glu.

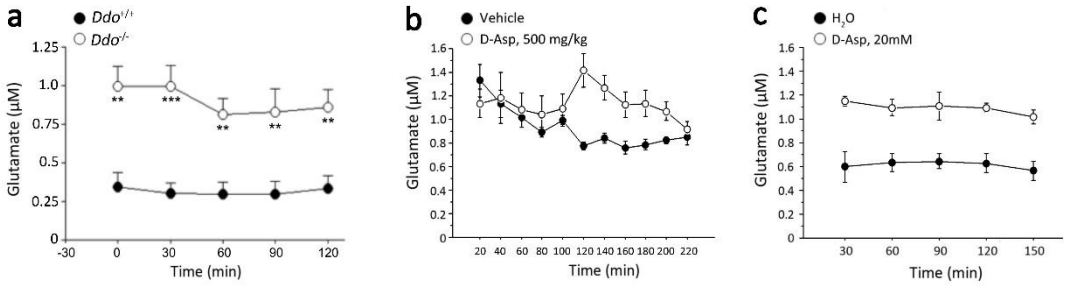

Figure 3.17: Increased D-Asp levels yields to a significant increase in the cortical extracellular levels of L-Glu. Cortical extracellular levels of L-Glu in (**a**) *Ddo*$^{+/+}$ and *Ddo*$^{-/-}$ mice, (**b**) control animals and mice subjected to the acute administration of 500 mg/kg of D-Asp, or (**c**) to the chronic oral treatment with 20 mM D-Asp. The graphs displayed the mean values±SEM; Significance was analyzed using two-way ANOVA with repeated measures followed by Fisher's post hoc test.

To comprehend the mechanism through which D-Asp triggers L-Glu release from glutamatergic nerve terminals, we isolated synaptic terminals from cerebrocortical neurons, called synaptosomes. On this preparation continuously superfused with a medium containing the non-selective excitatory amino acid transporter (EAAT) inhibitor TBOA (10 µM), we tested the ability of D-Asp to evoke L-Glu release, in the presence of K^+-induced depolarization. Spontaneous L-Glu levels were 21.3±1.1 nM (n=180), reported as zero in the graphic (Figure 3.18). A 90 s pulse with 15 mM K^+

caused a transient ~2.5-fold elevation of L-Glu levels over basal values, corresponding to a net release of 35.6±3.4 pmol/mg prot/min (Figure 3.18). D-Asp, L-Asp and NMDA (perfused at 10 μM) caused a similar ~3-fold elevation of the K^+-evoked L-Glu release [86.9±10.7, 112.1±12.4 and 106.9±15.4 pmol/mg prot/min, n=30, n=27, n=6, respectively; P<0.001; Figure 3.18a]. The effect of these agonists was differently sensitive towards subtype-selective L-Glu receptor antagonists (Figure 3.18). In fact, the non-competitive NMDAR antagonist MK-801 prevented the stimulation evoked by NMDA [treatment effect: $F_{(2,15)}$=12.61, P=0.0006; NMDA vs. NMDA + MK-801, P<0.01], attenuated that evoked by D-Asp [treatment effect: $F_{(2,26)}$=6.32, P=0.0058; D-Asp vs. D-Asp + MK-801, P<0.05] but left unchanged the response to L-Asp [treatment effect: $F_{(2,34)}$=6.97, P=0.0029; L-Asp vs. L-Asp + MK-801, P>0.05] (Figure 3.18a). Moreover, we treated synaptosomes with blockers of other Glu receptor as the ionotropic receptor AMPA and the metabotropic receptor mGluR5. Results showed that the AMPA receptor antagonist (CNQX) and mGluR5 antagonist (MTEP) prevented the effect of D-Asp [treatment effect: $F_{(3,56)}$=9.84, cerebrocortical P<0.0001; D-Asp vs. D-Asp + CNQX or D-Asp + MTEP P<0.01] but left unchanged that of L-Asp [treatment effect: $F_{(3,38)}$=10.23, P<0.0001; L-Asp vs. L-Asp + CNQX or L-Asp + MTEP P>0.05] (Figure 3.18b). Overall, this data revealed that D-Asp stimulates Glu release through presynaptic NMDA and non-NMDA ionotropic and metabotropic receptors.

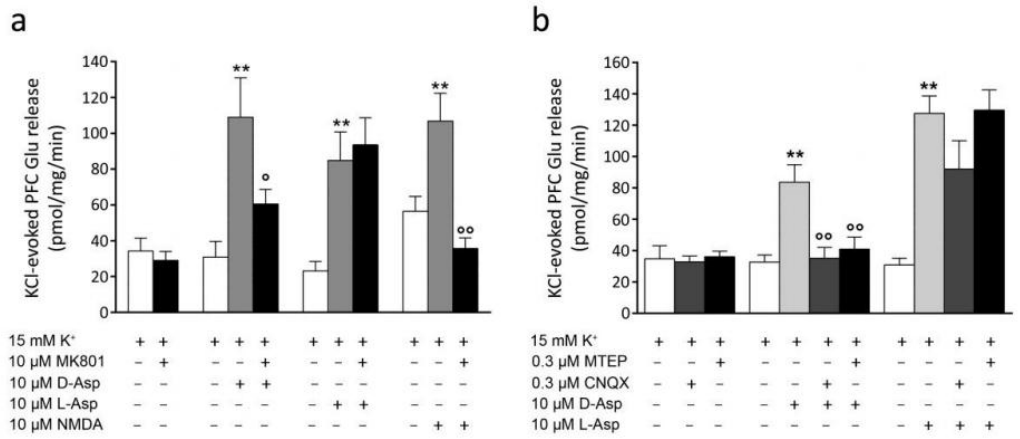

Figure 3.18: D-Asp stimulates L-Glu release from cerebrocortical synaptosomes through presynaptic NMDA and non-NMDA receptors. (**a, b**) Cerebrocortical synaptosomes were continuously perfused with a medium containing the EAAT inhibitor TBOA (10 μM), and stimulated with 15 mM K^+ for 90 sec. D-Asp, L-Asp and NMDA (10 μM) were added 3 min prior K^+ and maintained for further 3 min. MK-801 (**a**), CNQX or MTEP (**b**) were added 3 min before agonists and maintained until the end of experiment. Data represent net extra release (i.e. release above baseline), and are expressed as mean±SEM pmol/mg prot/min. ** P <0.01 different from K^+ alone, ° P <0.05, °° P <0.01 different from K^+ in the presence of agonist (one-way ANOVA followed by the Newman-Keuls test for multiple comparisons).

3.12 Effect of olanzapine on L-Glutamate, D-Aspartate and L-Aspartate extracellular levels

Several evidence has proved that second-generation antipsychotics influence glutamatergic system (Bakshi and Geyer, 1995; Duncan et al., 1999; Goff et al., 2002; Carli et al., 2011). In this light, we tested the effect of olanzapine, an atypical antipsychotic, on Glu extracellular levels in the PFC. To this aim, we treated C57BL/6 mice with i.p. injection of 5 mg/kg olanzapine for 4 weeks. Twenty-four hours after the last injection, we collected and analyzed dialysates using *in vivo* microdialysis approach. Interestingly, results showed a significant increase in L-Glu extracellular content in olanzapine-treated mice, compared to controls [two-way ANOVA with repeated measures, treatment effect: $F_{(1,16)}$=52.596, P=0.0019; Figure 3.19a]. Considering that also D-Asp is able to increase the cortical release of L-Glu (Figure 3.17), we examined whether olanzapine may influence extracellular content of D-Asp. Strikingly, chronic treatment with this antipsychotic drug caused a cortical increase of

extracellular free D-Asp [two-way ANOVA with repeated measures $F_{(1,16)}$=210.177, P=0.0001; Figure 3.19b]. Remarkably, we also detected augmented levels of this D-amino acid in total tissue extract of olanzapine-treated mice compared to untreated littermates [P=0.0064 Figure 3.19d]. Furthermore, our analysis revealed that chronic olanzapine administration also enhanced cortical extracellular L-Asp levels, although the increment was less than that of D-Asp [two-way ANOVA with repeated measures: $F_{(1,16)}$=45.837; P=0.0025; Figure 3.19c]. Unlike the D-Asp, no difference was found in L-Asp total level [P=0.6419; Figure 3.19e].

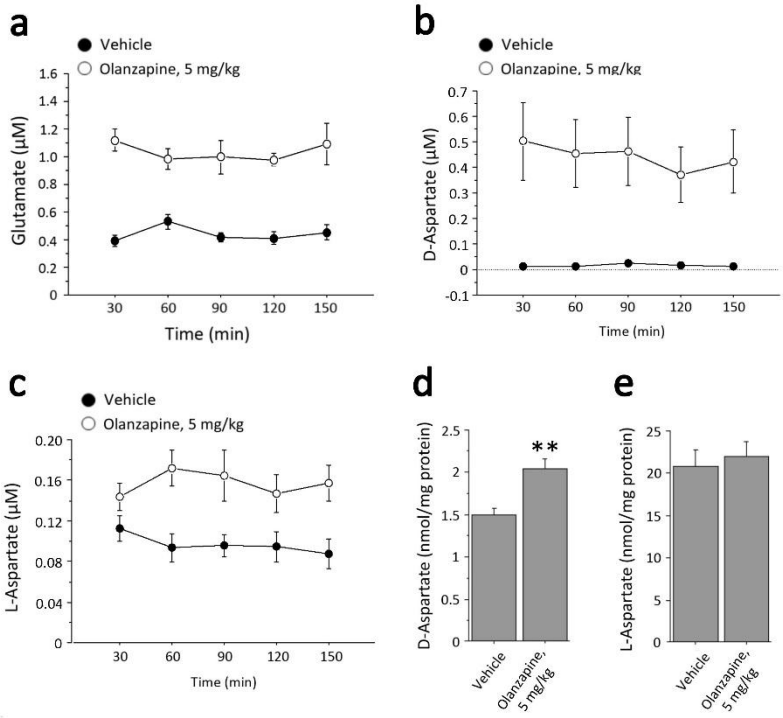

Figure 3.19: Olanzapine chronic administration triggers L-Glu release in the PFC and increases D-Asp total content and release. Free (**a**) L-Glu, (**b**) D-Asp and (**c**) L-Asp extracellular concentration in control animals and in mice subjected to the chronic administration of 5 mg/kg Olanzapine. Free (**d**) D-Asp and free (**e**) L-Asp total concentration in control and olanzapine treated mice. The amount of D-Asp and L-Asp in tissue homogenates was normalized by the total protein content of each sample. The graphs displayed the mean values ± SEM; ** P < 0.005 two-way ANOVA with repeated measures followed by Fisher's post hoc test for microdialysis analyses and Student's t-test for homogenates analyses.

3.13 Effect of Olanzapine on DDO activity

In the light of previously microdialysis results showing the ability of olanzapine to influence D-Asp levels in the homogenate fraction, we performed an

inhibition assay to assess if this antipsychotic drug could affect the activity of murine and human recombinant DDO (mDDO and hDDO, respectively). The assay was performed using different concentrations of antipsychotic (in the 0-300 μM range) at a fixed saturating concentration of exogenous FAD (100 μM). Interestingly, olanzapine was able to inhibit both mDDO and hDDO activity in a dose-dependent manner according to a classical sigmoidal dose-response curve (Figure 3.20a,b), with an IC50 value of 5.6±0.8 and 23.4±1.6 respectively. Notably, using a lower, physiological FAD concentration in the assay mixtures (4 μM), we observed a 4-fold increase in the inhibition efficiency of olanzapine on mDDO [IC50=1.4±0.2 μM; Figure 3.20a], whereas the IC50 value of hDDO was not affected [IC50=23.1±3.2 μM, Figure 3.20b]. Conversely, if we performed the same experiment with clozapine, another atypical antipsychotic, DDO activity did not changed (Figure 3.20c,d).

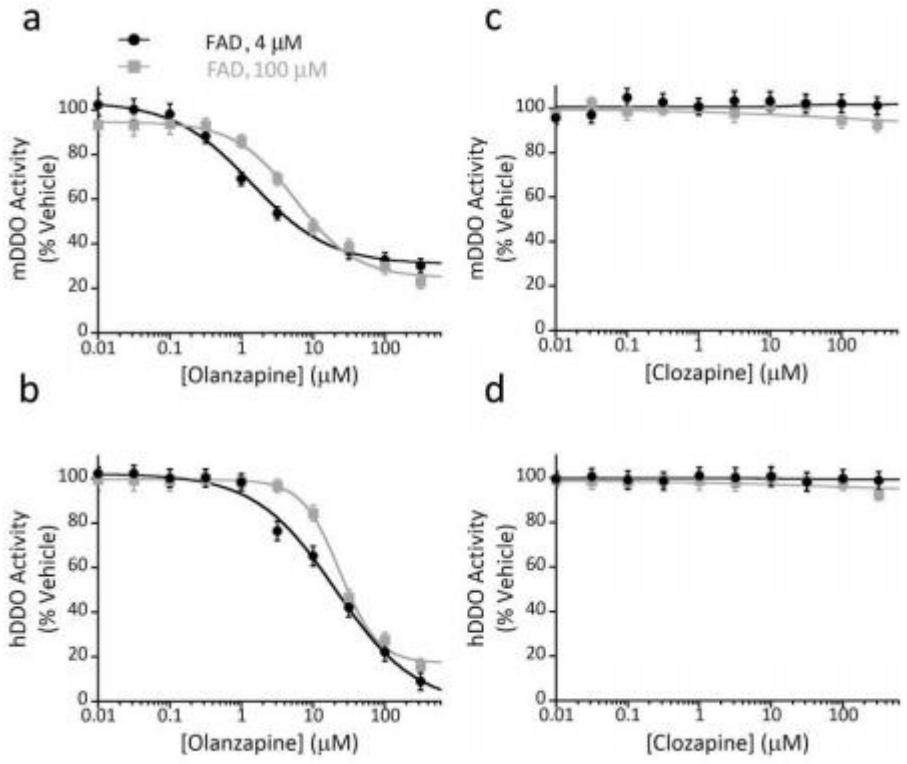

Figure 3.20: Olanzapine inhibits murine and human DDO activity. (**a-d**) Enzyme inhibition assays performed by using recombinant (**a, c**) mDDO or (**b, d**) hDDO and (**a, b**) olanzapine or (**c,d**) clozapine as inhibitors. DDO activity in the presence of different concentrations of the antipsychotics (in the 0-300 μM range) and two FAD concentrations (4 and 100 μM) was determined by the Amplex UltraRed assay and an automated liquid handler system. The plots display the mean values ± STD deviation. The IC50 values represent the olanzapine concentration required for 50% inhibition of the enzymatic activity.

4. Conclusion

D-Asp and D-Ser are the only two D-amino acids found in considerable amount in mammalian tissues, including the brain (Hashimoto and Oka, 1997). In the last years, intensive research has demonstrated that D-Ser is an endogenous co-activator at the strychnine-insensitive glycine site of NMDARs (Martineau et al., 2006; Billard, 2012) and that its metabolism is altered in SCZ patients (Hashimoto et al., 2003; Hashimoto et al., 2005), supporting a role for this D-amino acid in psychiatric disorders. Also D-Asp is known to bind and activate NMDARs (Errico et al., 2012). Moreover, electrophysiological and behavioural studies on animal models with increased levels of D-Asp have revealed a contribution of D-Asp in the regulation of NMDAR-dependent synaptic activity and function (Errico et al., 2012). The NMDAR is a specific type of ionotropic Glu receptor and forms a heterotetramer between two GluN1 and two GluN2 subunits. This type of Glu receptors has been implicated in the pathophysiology of SCZ (Javitt, 1987; Goff and Coyle, 2001; Sawa and Snyder, 2003; Coyle, 2012; Javitt, 2012). Previous study, in line with hypo-glutamatergic hypothesis of SCZ, revealed variable changes in the expression patterns of NMDAR subunits in the dorsolateral prefrontal cortex, depending on the cohorts of SCZ patients analysed (Sokolov, 1998; Dracheva et al., 2001), while no changes have been described in the caudate putamen (Dracheva et al., 2001). Therefore, we have analysed the expression of NMDAR subunits in *post-mortem* SCZ patients. Coherently, our experiments highlighted a significant decrease in GluN1, GluN2A and GluN2B in the prefrontal cortex but not in the caudate putamen of SCZ patients. Considering that D-Asp is able to modulate NMDAR function, along with the interest in potential therapies targeting D-amino acids in psychiatric disorders (refs), we evaluated the levels of D-Asp and its derivative, NMDA, in the *post-mortem* brains of SCZ patients. To this aim, we have used high-performance liquid chromatography (HPLC), based on the diastereomeric derivatization of samples. Interestingly, we found a consistent decrease in D-Asp levels, in both prefrontal cortex and caudate putamen of SCZ patients. Coherently, also its N-methyl-derivative, NMDA, is reduced in both regions analysed. The alteration of D-Asp levels does not depend by variation in the levels of its precursor, L-Asp, whose amount results unaltered. On the other hand, our neurochemical analysis revealed a mild but significant decrease in L-Glu content (12%) in the caudate

putamen, but not in the PFC of SCZ brains compared to healthy individuals. The reduction of D-Asp levels in SCZ samples correlates with increased expression of *DDO* gene, which encodes for the only enzyme known to catabolize D-Asp. In the absence of available antibodies selective for DDO, this evidence leaves us to hypothesize that the decreased levels of D-Asp in SCZ patients could be due to increased expression of the enzyme DDO. Finally, we revealed that alteration in *DDO* mRNA expression is not caused by epigenetic modifications in the methylation degree of CpG sites within the putative promoter of the *DDO* gene.

Overall, the results obtained in SCZ patients suggest a potential involvement of D-Asp in the pathophysiology of this psychiatric illness. Nevertheless, the biological significance and the relative functional contribution of reduced levels of D-Asp and NMDA in SCZ remain to be clarified. Therefore, we moved from humans to mouse models (Errico et al., 2006; Errico et al., 2008a; Errico et al., 2011b) to investigate whether non-physiological higher levels of D-Asp can affect SCZ-like phenotype and counteract SCZ-like behavioural and functional deficits induced by the psychotomimetic drug PCP. To this aim, we have developed a simple and rapid method for the simultaneous direct measurement of D-Asp, L-Asp and NMDA in brain tissue based on chiral fractionation of enantiamers and tandem mass spectrometry in multiple reaction monitoring (MRM) mode (LC-MS/MS). This method allowed us to detect D-Asp in the brain with greater sensitivity than HPLC previously used, and to correlate the amount of this D-amino acid with relevant pathophysiological processes. LC-MS/MS analysis confirmed what we have previously found by HPLC analysis (Errico et al., 2006; Errico et al., 2008a; Errico et al., 2011a), namely that the targeted deletion of the *Ddo* gene results in increased levels of D-Asp in the mouse brain, while no difference was found in L-Asp content. Analysis on mouse models with high levels of D-Asp revealed that the ability of this D-amino acid in activating the NMDA receptors is mirrored by increased dendritic arborization and spine density, and facilitated induction of late-phase LTP. Previous evidence indicates that storage of long-term memories is likely dependent on enhancement of long-term synaptic plasticity (Lamprecht R, LeDoux J. Structural plasticity and memory. Nat Rev Neurosci 2004; 5: 45–54). Thus, facilitation of L-LTP induced by higher levels of D-Asp is coherent with the improvement of cognitive abilities previously found in D-

Asp-treated and *Ddo*$^{-/-}$ mice (refs). Moreover, the block of L-LTP by cytochalasin D in mice with increased levels of D-Asp may suggest a potential effect of D-Asp on mTORC2 pathway since this complex is known to control actin polimerization and, in turn, the consolidation of long-term memories (Huang et al, Nat Neurosci, 2013). Remarkably, in serine racemase-deficient mice, reduction in D-Ser levels that results in NMDAR hypofunction, causes morphological defects, as well as alterations in mEPSCs and synaptic plasticity, paralleled by reduced mTOR signalling (Balu and Coyle, 2012; Balu et al., 2013). Several studies have linked altered metabolism of the endogenous NMDAR co-agonist D-Ser to the etiopathology of SCZ (Hashimoto et al., 2003; Hashimoto et al., 2005; Yamada et al., 2005). The functional and structural similarities between D-Ser and D-Asp strengthen the hypothesis of a potential convergence of D-Asp on SCZ pathophysiology.

To evaluate in a preclinical model the effect of an altered metabolism of D-Asp on SCZ-like manifestations, we tested psychotic-like effect of PCP in *Ddo*$^{-/-}$ mice. This drug induces SCZ-like psychotic effects by blocking NMDARs (Javitt, 1987; Javitt et al., 2012; Moghaddam and Krystal, 2012). We found significantly reduced psychostimulant effect of PCP in *Ddo*$^{-/-}$ mice, as shown by their attenuated motor hyperactivity, compared with control littermates. Most importantly, constitutively increased levels of D-Asp in knockout animals also produced a reduced sensitivity to PCP-dependent disruption of sensorimotor gating. As the PPI paradigm is used as an endophenotypic trait to assess dysfunction of sensorimotor gating processing in SCZ patients (Gottesman and Gould, 2003), the modulation of PCP-induced disruption of PPI in animals characterized by elevated D-Asp levels is of potential translational relevance. In line with behavioral data, fMRI results show that increased D-Asp, through its ability to promote NMDAR transmission, strongly inhibited the functional activation elicited by PCP in cortico–limbo–thalamic regions of *Ddo*$^{-/-}$ mice. This effect is consistent with previous imaging work showing that pharmacological potentiation of NMDAR function by D-Ser, can effectively inhibit the hyperglutamatergic state produced by NMDAR antagonism (Gozzi et al., 2008c) and modulate psychosis-related neurocircuits. Interestingly, oral supplementation of a neurobiologically active dose of D-Asp to adult C57BL/6 mice failed to inhibit PCP-induced behavioral or functional responses. These findings point at a putative

neurodevelopmental origin for some of the phenotypes observed in *Ddo*$^{-/-}$ mice and suggests that both the time window and duration of increased D-Asp could have a critical role in shaping NMDAR-mediated circuit responsivity.

To better understand how exogenous D-Asp influences NMDAR function and SCZ-related phenotypes, we analysed the effects of D-Asp administration on the exogenous levels of this D-amino acid. First, we revealed that acute injection of D-Asp rapidly enhances the extracellular levels of free D-Asp in the PFC of freely moving mice, proving the evidence that exogenous D-Asp can efficiently cross the blood brain barrier. As after acute injection, we found that also chronic oral administration of D-Asp is able to enhance the extracellular levels of this D-amino acid in the mouse PFC. Furthermore, we demonstrated that this release occurs through a Ca^{2+}-dependent process, since without Ca^{2+} the extracellular content of D-Asp becomes undetectable. Such result is in accordance to previous *in vitro* findings showing that D-Asp can be released through vesicular Ca^{2+}-mediated exocytosis (Davies and Johnston, 1976; Malthe-Sorenssen et al., 1979; Wolosker et al., 2000; Nakatsuka et al., 2001; D'Aniello et al., 2010). Remarkably, we found that both acute and chronic D-Asp treatment is able to increase the extracellular levels of L-Glu in freely moving mice. In this regard, using synaptosomal preparation from mouse PFC, we also revealed that D-Asp, but not L-Asp, stimulates presynaptic L-Glu release acting on NMDA, AMPA/kainate and mGluR5 receptors, suggesting that D-Asp could activate NMDAR both directly and indirectly by promoting Glu release.

As D-Asp, also the second-generation antipsychotic olanzapine is able to affect glutamatergic system (refs). Interestingly, we have found that olanzapine is able to increase extracellular D-Asp levels in the PFC of treated mice due to its ability to inhibit DDO activity, as demonstrated by in vitro assays with both human and mouse recombinant enzymes. Altogether, our results highlight an unexpected role for olanzapine in the modulation of free D-Asp metabolism and lead us to hypothesize that the reported increase of the endogenous extracellular D-Asp may be one of the mechanisms by which this antipsychotic influences glutamatergic neurotransmission.

Taken together, these findings support a role for D-Asp in phenotypes relevant to SCZ. Consistent with a neurodevelopmental hypothesis of SCZ (Fatemi and Folsom, 2009; Owen et al., 2011), a putative precocious down regulation of D-Asp levels, associated

to abnormal metabolism of this molecule, may have a much greater impact during critical phases of brain development, when D-Asp levels are physiologically high (Hashimoto et al., 1993; Sakai et al., 1998; Wolosker et al., 2000). Moreover, our results and previous evidence suggest that this D-amino acid, like D-Ser (Tsai et al., 1998; Hashimoto et al., 2013; Balu and Coyle, 2015), may prove to be beneficial also in humans and could be potentially tested as an add-on to antipsychotics for schizophrenia treatment. Future studies in mouse models permitting controlled exposure of D-Asp levels during neurodevelopment will be made to investigate this basic issue.

5. Materials and Methods

5.1 Tissue collection

Prefrontal cortex and caudate putamen samples from *post-mortem* brains of non-psychiatrically ill individuals (controls) and subjects with SCZ were obtained from the brain bank of the Institute of Psychiatry, King's College London, UK. All tissue collection and processing was carried out under the regulations and licences of the Human Tissue Authority and in accordance with the Human Tissue Act of 2004. Clinical diagnosis of SCZ was performed according to DSMIII-R criteria. Demographic characteristics of the control and SCZ subjects are described in Table 5.1. The analyses of age, gender and *post-mortem* interval effects between the two groups are shown separately for each experiment in the next sections.

Control					Schizophrenia					
Nr	Gender	Age (years)	PMD (h)	Cause of death	Nr	Gender	Age (years)	PMD (h)	Antipsychotic used	Cause of death
1	Female	52	44	Carcinoma of the lung	16	Male	79	48	Promazine	Cardiac arrest
2	Male	61	53	Cardiac arrest	17	Female	70	100	Trifluoperazine	Bronchopneumonia
3	Female	76	28	Congestive cardiac failure	18	Female	69	?	?	?
4	Female	80	31	Left ventricular failure/bronchopneumonia	19	Male	62	36	Carbamazepine	Pulmonary tuberculosis
5	Male	86	6	Myocardial infarction	20	Female	76	97	Haloperidol	Bronchopneumonia
6	Male	65	24	Coronary artery occlusion	21	Female	49	100	?	Perforated duodenal ulcer
7	Female	68	9	Cardiac arrest	22	Male	31	27	Chlorpromazine	Multiple organ failure
8	Female	26	10	Hepatic necrosis	23	Male	51	44	Thioridazine, fluphenazine	Myocardial infarction
9	Male	37	27	Acute necrotic pancreatitis	24	Male	64	48	?	Acute liver failure
10	Male	49	32	Coronary artery occlusion	25	Female	84	42	Haloperidol	Bronchopneumonia
11	Male	49	44	Pulmonary oedema	26	Male	87	48	Stelazine	Bronchopneumonia
12	Male	80	35	Left ventricular failure	27	Female	32	46	Chlorpromazine	Pulmonary embolism
13	Female	62	88	Haemothorax	28	Male	35	67	Flupenthixol	Bronchopneumonia
14	Female	73	70	Pelvic carcinoma	29	Female	75	50	Trifluoperazine	Myocardial infarction
15	Male	85	42	Gastrointestinal haemorrhage	30	Male	62	48	?	Ischaemic heart disease

Table 5.1: Demographic and clinical characteristics of deceased schizophrenic and control subjects. Tissue samples were obtained from the brain bank of the Institute of Psychiatry, King's College London, UK. Gender, age (years), post-mortem delay (h) and the cause of death of each individual are indicated. The antipsychotics used by schizophrenic patients are also reported. Nr = number; PMD = post-mortem delay; ? = unknown.

5.2 HPLC analysis on human samples

Prefrontal cortex and caudate putamen samples from post-mortem brains of 7 controls and 10 subjects with SCZ were used to evaluate the levels of D-Asp, NMDA, L-Asp and L-Glu. The two groups were matched for age [control vs. SCZ, 62.6±7.4 years vs.63.2±6.1years, p=0.9484; Student's t test], gender (χ2 test: 0.26) and post-mortem delay [control vs. SCZ, 34.9±9.2 h vs. 51.1±7.1 h, p=0.1756; Student's t test].

To detect D-Asp, NMDA, L-Asp and L-Glu, tissue samples were purified according to a previously described procedure (D'Aniello et al., 2000). Briefly, each tissue was homogenized 1:10 (w:vol) in 0.05 M phosphate buffer pH 7.4 in presence of protease inhibitors and centrifuged at 3000 rpm for 10 min. The supernatant was further centrifuged at 14.000 rpm for 20 min and the supernatant was treated with 1 vol of 0.2 M TCA. The sample was recentrifuged as above and the supernatant applied to the cation exchange AG 50 W-X8 resin (Bio-Rad). The eluate was utilized for HPLC determination of D-Asp, L-Asp, L-Glu and NMDA as described previously (D'Aniello et al., 2005). For D-Asp, L-Asp and L-Glu detection, 20 µl of each sample were added to a mixture consisting of 0.04M pyrophosphate buffer pH 9.5, 2 µg/µl OPA (o-phthaldialdehyde) and 1 µg/µl NAC (N-acetyl cysteine) to a final volume of 500 µl and 50 µl were loaded on HPLC column, after 2 min of incubation. The same procedure was followed for a standard mixture of 17 L-amino acids plus D-aspartic acid. In this case 0.05 nmol of each L-amino acid plus 0.025 nmol of D-Asp were injected. The column was eluted at 1.2 ml/min, with a gradient consisting of solution A (920 ml of water, 30 ml of 1 M citrate/phosphate buffer (McIlvaine buffer), pH 5.6, and 50 ml of acetonitrile) and solution B (90% acetonitrile in water). The program gradient was 0–5% solution B for 10 min; 5–30% solution B for 30 min, 30–100%solution B for 10 min, staying at 100%solution B for 5 min and returning to 0% of solution B for 1 min. The fluorescence was read at an excitation wavelength of 330 nm and an emission wavelength of 450 nm. D-Asp was eluted with a peak at 5.6 min, followed by L-Asp 0.5 min later and L-Glu about 1 minute later and was well separated from other amino acids. To verify that the peak eluted at 5.6 min was really D-Asp, 10 µl of the sample was mixed with 20 µl of 0.5 M pyrophosphate buffer, pH 8.2, and 2 µl of purified DDO, and incubated for 20 min at 37◦C, then 100 µl of 0.5 M pyrophosphate buffer, pH 9.5, and 20 µl of OPA/ NAC were added, before HPLC, as described above. The absence of the peak at elution time 5.6 min or its decrease confirmed the presence of D-Asp. The standard mixture of amino acids was carried out under the same conditions to give a standard curve. The areas of the peaks of amino acid standards were used to calculate the amount of D-Asp and other amino acids contained in the sample. NMDA do not have a primary amino group, so it do not react with OPA and are eluted immediately from the C-18column. Therefore, to detect the

content of NMDA we used a method based on the measurement of the CH_3-NH_2 (methylamine), which is generated from the reaction between NMDA and DDO (D'Aniello et al., 2000), as shown by the following reaction:

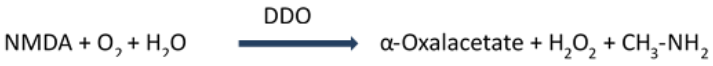

Therefore, for NMDA detection, 75 µl of each sample were incubated with 2 µl of bovine DDO (1 µg /µl), in presence of 10 µl of 1M borate buffer pH 8.0, for 30 min at 37°C. After incubation, to each sample is added 0.4 M borate buffer pH 9.5 to a final volume of 135 µl and then 15 µl of OPA-mercaptoethanol reagent (consisting of 5 mg OPA in 1 ml methanol and 10 µl of β-mercaptoethanol). After 2 min (needed to obtain the complete derivatization of the amino acids), 100 µl of sample was injected onto a C-18 Supelcosil HPLC column, using the Beckman-Gold HPLC system. The column was eluted with a gradient consisting of solvent A (10% acetonitrile in 30 mM sodium acetate buffer, pH 5.5) and solvent B (70% acetonitrile in 30 mM sodium acetate buffer, pH 5.5) using the following gradient program: 0–40% B over 15 min; to 100% B in 4 min, staying at 100% B for 3 min and back 0% B in 1 min, at a flow rate of 1.2 ml/min. CH3-NH2 was detected fluorometrically at an excitation wavelength of 330 nm and an emission wavelength of 450 nm. The CH_3-NH_2 eluted as a sharp peak at the retention time of 21.2 min, well separated from the other amino acids. After running the sample, 5 ml of OPA-mercaptoethanol was added to the blank sample, consisting of 20 ml of sample as purified above and 20 ml of 0.1 M borate buffer, pH 8.2, and chromatographed as with the sample. The difference of the peak areas obtained between the sample and the blank sample gave the net amount of the area due to the methylamine generated by the action with DDO. To quantify the concentration of NMDA in the sample, a standard curve of different concentrations of NMDA (range 0.1–1.0 nmol/ml) was performed under the same assay conditions as the samples.

5.3 Western blotting

Frozen, powdered PFC and caudate-putamen samples from post-mortem brains were sonicated in 1% SDS and boiled for 10 min. Aliquots (2 µl) of the homogenates were used for determination of total proteins using Bio-Rad Protein Assay dye. Equal

amounts of total proteins (35 μg) for each sample were loaded onto 10% polyacrylamide gels. Proteins were separated by SDS-PAGE and transferred overnight to membranes (polyvinylidene difluoride) (GE Healthcare). Membranes were immunoblotted using antibodies against GluN1, GluN2A (1:1000, Sigma, St. Louis, MO, USA), GluN2B (1:1000, Millipore, Billerica, MA, USA) and GAPDH (1:1000, Santa Cruz Biotechnology, Santa Cruz, CA, USA). Blots were then incubated in horseradish peroxidase-conjugated secondary antibodies. Target proteins were visualized by ECL detection (Pierce) and quantified by Quantity One software (Bio-Rad). Optical density values were normalized to GAPDH for variations in loading and transfer. Means and SEM of normalized values were then compared using non-parametric Mann-Whitney test. The analysis of GluN1 was performed on 15 control and 14 SCZ subjects in the prefrontal cortex and on 14 control and 13 SCZ subjects in the caudate putamen. In both brain areas, the two groups were matched for age [prefrontal cortex: control vs. SCZ (mean±SEM), 63.3±4.6 years vs. 61.7±5.1 years, p=0.8228; caudate putamen: control vs. SCZ (mean±SEM), 64.3±4.8 years vs. 60.4±5.3 years, p=0.5913; Student's t test] and gender (χ^2 test: prefrontal cortex, 0.86; caudate putamen, 0.84). The *post-mortem* delay was significantly longer in SCZ patients compared to the control group [prefrontal cortex: control vs. SCZ (mean±SEM), 35.1±5.7 h vs. 58.8±6.8 h, p=0.0120; caudate putamen: control vs. SCZ (mean±SEM), 35.3±6.1 h vs. 58.7±7.5 h, p=0.0223; Student's t test]. The analysis of GluN2A was performed on 15 control and 15 SCZ subjects in the prefrontal cortex and on 15 control and 12 SCZ subjects in the caudate putamen. In both brain regions, the two groups were matched for age [prefrontal cortex: control vs. SCZ (mean±SEM), 63.3±4.6 years vs. 61.7±4.8 years, p=0.8186; caudate putamen: control vs. SCZ (mean±SEM), 63.3±4.6 years vs. 61.3±5.7 years, p=0.7918; Student's t test] and gender (χ^2 test: prefrontal cortex, 1; caudate putamen, 0.86). The *post-mortem* delay was significantly greater in SCZ patients, compared to control group [prefrontal cortex: control vs. SCZ (mean±SEM), 35.1±5.7 h vs. 57.2±6.5 h, p=0.0160; caudate putamen: control vs. SCZ (mean±SEM), 35.1±5.7 h vs.55.0±7.1 h, p=0.0374; Student's t test]. The analysis of GluN2B was performed on 11 control and 10 SCZ subjects in the prefrontal cortex and on 6 control and 4 SCZ subjects in the caudate putamen. In the caudate putamen, the two groups were matched for age [control vs.

SCZ (mean±SEM), 76.3±4.2 years vs. 67.2 ±2.4 years, p=0.4373; Student's t test], gender (χ^2 test: 0.60) and *post-mortem* delay [control vs.SCZ (mean±SEM), 36.5±10.2 h vs.55.5±14.8 h, p=0.3042; Student's t test]. In the prefrontal cortex, control and SCZ groups were matched for gender (χ^2 test: 0.80), while age of SCZ subjects was significantly younger and the *post-mortem* delay significantly longer compared to the respective control groups [age effect: control vs. SCZ (mean±SEM), 71.6±3.3 years vs. 56.1±5.7 years, p=0.0254; *post-mortem* delay effect: control vs. SCZ (mean±SEM), 38.4±7.0 h vs .63.4±9.6 h, p=0.0450; Student's t test].

5.4 Quantitative reverse transcription-polymerase chain reaction analysis in humans

Total RNA was extracted using miRNeasy® kit (Quiagen, Hilden, Germany) according to the manufacturer's instructions. RIN of samples was assessed using Biorad Experion Automated electrophoresis Station (Hercules, CA) prior to cDNA synthesis with Transcriptor First Strand cDNA Synthesis kit (Roche Diagnostics, Mannheim, Germany). Total RNA (0.5 μg per sample) was used to synthesize cDNA. Quantitative RT-PCR with Real Time ready catalog Assays (Roche Diagnostics) and LightCycler® 480 Probe Master (Roche Diagnostics) was performed on a Light Cycler 480 II Real Time PCR system with 96-well format (Roche Diagnostics). All measurements from each subject were performed in duplicate. DDO mRNA expression levels were normalized to the geometric mean of three housekeeping genes: β-actin, glyceraldehyde-3-phosphate dehydrogenase (GAPDH), and cyclophilin (PPIA). The following primers were used for DDO cDNA amplification: DDO fw 5'-GGTGTTCATTTGGTATCAGGTTG-3' and DDO rev 5'-TTTCGAAATCCCAGAACCA-3'; β-actin fw 5'- TCCTCCCTGGAGAAGAGCTA-3' and β-actin rev 5'-CGTGGATGCCACAGGACT-3'; GAPDH fw 5'-AGCCACATCGCTCAGACAC -3' and GAPDH rev 5'-GCCCAATACGACCAAATCC -3'; PPIA fw 5'-TTCATCTGCACTGCCAAGAC -3' and PPIA rev 5'- CACTTTGCCAAACACCACAT -3'. Changes in DDO mRNA expression of SCZ, compared with Ctrl, were calculated using the relative

quantification method ($2^{-\Delta\Delta Ct}$) and used as dependent variable. Data were analyzed using analysis of covariance with diagnosis as the predictor. *Postmortem* delay was modeled as covariate of no interest.

5.5 Methylation analysis

Methylation status of the putative DDO promoter was assessed through a strategy on the basis of the locus-specific amplification of bisulfite-treated genomic DNA. Sodium bisulfite conversion was performed by using EZ DNA Methylation Kit (Zymo Research). The manufacture's protocol was followed by using 2 µg of genomic DNA and eluted in 30 µl of H_2O. The average conversion rate was 99.1%. Methylation status was assessed through a strategy based on the locus-specific amplification of bisulfite-treated genomic DNA, amplifying each amplicon separately, followed by Roche 454 resequencing. Fusion primers were designed to generate tiled amplicons ranging in size between 300-400 bp segments. Fusion primers used for this analysis were: DDO fw 5'-aTTtaTaaatTagTtggagaaagTTTag-3' and DDO rev 5'-cacaAtAAcctAtccatcactAtcc-3' (where the capital letters indicate the original C or G, respectively). At the 5′ end, fusion primers contained an additional sequence, MID, that barcodes the sample. The MID sequence was selected from a list provided from Roche. Thermal cycling was performed as follows: one cycle at 95 °C for 2 min followed by 40 cycles at 95 °C for 30 s, at the specific annealing temperature for 30 s, at 72 °C for 50 s, followed by a final extension step at 72 °C for 6 min. Small DNA fragments were removed using AMPure PCR purification system (Agencourt, Beverly, MA, USA) following the manufacturer's protocol. Amplicons were quantified using the Quant-iT PicoGreen dsDNA reagent (Invitrogen Corporation, Life Techologies, Carlsbad, CA, USA). All amplicons were pooled at an equimolar ratio and the sample pool was diluted to a final concentration of 1×10^7 PCR molecules/µl. The amplicon fragments were annealed to carrier beads and clonally amplified by emulsion PCR (emPCR). emPCR was performed according to the manufacturer's protocol. The beads were isolated and compartmentalized into droplets of an aqueous PCR reaction buffer in oil emulsion. Subsequently, the emulsions were

broken by isopropanol to facilitate collection of the amplified fragments bound to their specific beads. The beads carrying single-stranded DNA templates were enriched, counted and deposited into the PicoTiterPlate for sequencing. Data analysis was performed using the Roche proprietary software package for the GS Junior system. Post-run analysis was conducted using the version 2.7 of GS Amplicon Variant Analyzer. In this study, amplicon nucleotide sequence reads were aligned to the human genomic sequence of DDO. The AVA software identified all nucleotide variants, and provided read counts and frequencies. Individual flow grams were reviewed to examine and confirm all variant calls made by the software. Methylation analysis of one patient and one control subject gave no results and thus were excluded. The average number of molecules analyzed for subject was 207/sample for a total number of 11.818 reads. Data were analyzed using analysis of covariance with diagnosis as the predictor. *Postmortem* delay was modeled as covariate of no interest.

5.6 Animals

Knockout male mice for the *Ddo* gene were generated and genotyped by PCR as described previously (Errico et al., 2006). C57BL/6J male mice were purchased from the Jackson Laboratory (Bar Harbour, ME, USA). Animals were either chronically administered with D-Asp by delivering the D-amino acid (20 mM) in drinking water for 1 month, or acutely administered by intra-peritoneal (i.p.) injection (500 mg/kg D-Asp, dissolved in 0.9% NaCl). Animals were group housed (five per cage), at a constant temperature (22±1 °C) on a 12 h light/dark cycle (lights on at 7 AM) with food and water ad libitum. All research involving animals was carried out in accordance with the European directive 86/609/EEC governing animal welfare and protection, which is acknowledged by the Italian Legislative Decree no. 116, 27 January 1992. Every effort was made to minimize suffering of the animals. Animal research protocols were also reviewed and consented to by a local animal care committee.

5.7 LC-MS/MS

All molecules were purchased from Sigma-Aldrich. All the solutions and solvents were of the highest available purity and were suitable for LC–MS analysis and purchased from J. T. Baker (Phillipsburg, NJ). All stock solutions were stored at −20 °C. Tissue samples derive from *Ddo*$^{-/-}$ mice.

The spiking standard was prepared by adding 1.00 mL aliquots of each molecule to a 10-mL volumetric flask and bringing the standard to volume with methanol to yield a standard with 1000 ng/mL of each molecule. The spiking standard should be stored at −20 °C until the analysis. This was used to correct the recoveries of the different analytes.

Stock solutions were prepared, for each metabolite standard at a concentration of 1.0 mg/mL in methanol. Final 2 μg/mL individual metabolite standard solutions were prepared, by serious dilution from stock, and were used for mass spectrometric tuning. A standard mixture of all metabolites at 5, 10, 25, 50, 100, 200, 300, 500 pg/ul for metabolites having higher, medium, and lower measuring sensitivities, respectively, under current experimental condition, was prepared, from individual standard stock solution, and then used to generate lower concentration levels via series dilutions for linearity assessment.

All tissues were homogenized by sonication in Tris buffer pH 8, and stored at −20 °C until the time of analysis. For an initial screening extraction batch run, the control tissue was fortified in triplicate at the 200 pg/ul target level by adding the spiking standard solution to a 4.0-g portion of control tissue. Aliquot of 0.6 ml of methanol was added (0.2ml) to each sample and the tube was mechanically shaken vigorously for 5 min. The tube was centrifuged at 10000 rpm (7600 rcf) at 10 C for 10 min. Using a Pasteur pipette, the upper organic layer was transferred into a centrifuge tube. 0.2ml of upper organic layer was filtered through a 0.2-μm PTFE syringe filter (Pall Acrodisc 13 mm) into an LC vial for analysis.

Two ul of supernantant were analysed by using a 6420 triple Q system with a HPLC 1100 series binary pump (Agilent, Waldbronn, Germany). The enantiomers were separated by using as analytical column an Astec chirobiotic T column 10 cm x 4,6mm, 5u. The mobile phase was generated by mixing eluent A (0.1 % Formic Acid in 2%

ACN) and eluent B (0.009 % Formic Acid in methanol) and the flow rate was 0.500 mL/min. Starting condition was 50% to 95% B in 6 min.

Tandem mass spectrometry was performed using a turbo ion spray source operated in positive mode, and the multiple reaction monitoring (MRM) mode was used for the selected analytes. A standard solution of 500 pg/ul of each metabolite was used for optimization of the MRM transition reported in Table 5.1.

Compound Name	Precursor Ion	Product Ion
Aspartic acid	134.1	116
	134.1	88
	134.1	74

Table 5.1: MRM transition

Metabolites were automatically (flow injection) tuned for ionization polarity, optimal declustering potential (DP), product ion, and collision energy (CE) using metabolite standard solutions via Agilent MassHunter Optimizer software. Table 5.1 provides a list of precursor ion, product ions, collision energy and retention times for all analytes. Extracted mass chromatogram peaks of metabolites were integrated using Agilent MassHunter Quantitative Analysis software (B.05.00). Peak areas of corresponding metabolites are then used, as quantitative measurements, for assay performance assessments such as assay variation, linearity etc.

5.8 Golgi-Cox staining and dendritic spine measurements

Golgi-Cox staining was performed on brains of naive animals, according to a previous protocol (D'Amelio et al., 2011). Fully impregnated pyramidal neurons laying in the PFC and in the CA1 region of the dorsal hippocampus were visualized at × 100 (oil-immersion) using a microscope (DMLB, Leica Biosystems) equipped with a camera (resolution = 2600 × 2600, Axiocam, Zeiss AG, Oberkochen, Germany), and the KS300 3.0 system (Zeiss). A computer-based neuron tracing system (Neurolucida, Microbrightfield, MBF Bioscience, Williston, VT, USA) was used to trace single neurons. Total dendritic length and spine density were calculated according to D'Amelio et al., 2011 and analyzed using Student's t-test. Dendritic complexity was calculated according to Balu et al. (Balu and Coyle, 2012) and analyzed using two-

way analysis of variance with repeated measures, followed by Fisher's *post hoc* comparison when required.

5.9 Electrophysiology

Coronal slices from mouse medial PFC (mPFC; 250μm) were cut in ice-cold artificial cerebrospinal fluid using standard procedures. Visually guided whole-cell recordings were performed as previously described (Nistico R, Mango D, Mandolesi G, Piccinin S, Berretta N, Pignatelli M et al. Inflammation subverts hippocampal synaptic plasticity in experimental multiple sclerosis.PLoS One2013;8: e54666) using 1.5 mm borosilicate glass electrodes (3–4MΩ) filled with a solution containing (in mM) $CsMeSO_4$(130), HEPES (5.0), EGTA (0.5), $MgCl_2$(1.0), NaCl (1.0), $CaCl_2$(0.34), QX-314 (5.0), adjusted to pH 7.3 with CsOH. Miniature excitatory postsynaptic currents (mEPSCs) were collected from layer II/III mPFC pyramidal neurons and NMDA currents were pharmacologically isolated according to a previously described procedure (Rompala GR, Zsiros V, Zhang S, Kolata SM, Nakazawa K. Contribution of NMDA receptor hypofunction in prefrontal and cortical excitatory neurons to schizophrenia-like phenotypes.PLoS One2013;8: e61278).For extracellular recordings, parasagittal hippocampal slices (thickness, 400μm) were cut using a Vibratome (Leica VT1000 S, Leica Biosystems, Wetzlar, Germany). Slices were incubated for 1 h in a holding chamber and then transferred to a recording chamber, completely submerged in artificial cerebrospinal fluid (30–31 °C) of the following composition (in mM): NaCl (124), KCl (3.0), $MgCl_2$ (1.0), $CaCl_2$(2.0), $NaH2PO_4$(1.25), $NaHCO_3$ (26), glucose (10); saturated with 95% O_2, 5% CO_2. Bipolar stimulating electrodes placed in the stratum radiatum to activate the Schaffer collateral commissuralfibers. Recordings offield excitatory postsynaptic potentials were made in the middle of the stratum radiatum by using microelectrodesfilled with artificial cerebrospinalfluid (resistance 3–5MΩ). LTP was induced with 1 s, 100 Hz stimulation. For statistical analysis we used unpaired t-tests after LTP induction (on the average of the last 10 min of recording).

5.10 PCP-induced motor activity

The procedure used has been previously described (Errico et al., 2008a). PCP (Sigma, St Louis, MO, USA) was dissolved in distilled water at the dose of 3 and 6 mg/kg in a volume of 10 ml/kg. After 1 h of habituation to the test cage (35 × 25 × 30 cm), PCP (3 and 6 mg/kg) or vehicle were injected intraperitoneally to male 3-month-old *Ddo*$^{+/+}$ and *Ddo*$^{-/-}$ mice and locomotion, expressed in cm, recorded over 1 h by using a computerized video tracking system (Videotrack; Viewpoint, Lyon, France). Motor response to PCP was evaluated by three-way analysis of variance (ANOVA; genotype × treatment × time) with repeated measures, followed by twoway ANOVA (genotype × time) with repeated measures.

5.11 Prepulse inhibition of the startle reflex under PCP treatment

Ddo$^{-/-}$ and D-Asp-treated mice, and their respective control groups (*Ddo*$^{+/+}$ and H_2O-treated mice, respectively), were assigned to receive either PCP (3 and 6 mg/kg) or vehicle (balanced for genotype and startle chamber assignment) and placed in a Plexiglas cylinder within the startle chamber 10 min after intraperitoneal injection. Prepulse inhibition (PPI) was measured using an SR-Lab System as previously described (Errico et al., 2008c). We chose to test 70, 74, 78 and 82 dB prepulse sounds (5, 9, 13 and 17 dB above background, respectively). PPI data were analyzed within genotype using two-way ANOVA (treatment × prepulse sound levels) with repeated measures.

5.12 Functional and pharmacological magnetic resonance imaging

Resting-state and pharmacological functional magnetic resonance imaging (fMRI) (Ferrari et al., 2012; Sforazzini et al., 2014)were performed on male 3–4-month-old *Ddo*$^{-/-}$ mice (n=9) and *Ddo*$^{+/+}$ littermates (n= 12). An additional pharmacological fMRI study was carried out on 4-month-old male C57BL/6-J mice treated with D-Asp (n= 10) or water (n= 10) for 1 month. Briefly, mice were intubated, artificially ventilated and imaged under halothane (0.7%) anesthesia. Mean blood pressure, p_aCO_2 and p_aO_2 levels were recorded to rule out non-physiological states. MRI acquisitions were carried out at 7.0 Tesla. For each session, high-resolution

anatomical images were followed by a co-centered single-shot BOLD fMRI time series. The functional effect of PCP was mapped using a pharmacological fMRI as previously described (Gozzi et al., 2008c; Gozzi et al., 2008b; Dodero et al., 2013). fMRI time series were sensitized to cerebral blood volume using a blood-pool contrast agent, and 15 min later each subject received an intra-arterial injection of PCP (1 mg/kg). To assess the modulatory role of D-Asp elevation in wild-type mice, an additional pharmacological fMRI study with PCP was performed in C57BL/6-J mice exposed to D-Asp (20 mM in tap water) or vehicle (plain water) for 1 month (n= 10 each group). Inter-strain differences in resting-state fMRI (rsfMRI) correlation networks were mapped and quantified using a seed-based approach as recently described (Sforazzini et al., 2014; Zhan et al., 2014). Small *a priori* seed regions were chosen to cover antero–posterior cortical and hippocampal networks. The fMRI response to PCP was mapped and quantified as previously described (Gozzi et al., 2008c; Gozzi et al., 2008b; Gozzi et al., 2008a). Relative cerebral blood volume time series before (8 min) and after drug or vehicle injections (24 min) were extracted and voxel-wise group statistics were performed using FEAT Version 5.63 with 0.5 mm spatial smoothing and family-wise cluster correction threshold of 0.001.

5.13 *In vivo* microdialysis

Microdialysis experiments were performed in awake and freely moving mice as previously reported (Guida et al., 2015). Briefly, 3/4-month-old C57BL/6J mice were anaesthetized with pentobarbital (50 mg/kg, i.p.) and stereotaxically implanted with concentric microdialysis probes into the PFC using the following coordinates AP: 1.8 mm; L: 0.4 mm from bregma and V: 3.0 mm below the dura, and secured to the skull using stainless steel screws and dental cement. Microdialysis probes were constructed with 22G (0.41 mm I.D., 0.7 mm O.D.) stainless steel tubing: inlet and outlet cannulae (0.04 mm I.D., 0.14 mm O.D.) consisted of fused silica tubing. The probe had a tubular dialysis membrane (Enka AG, Wuppertal, Germany) 1.3 mm in length. After a post-operative recovery period of 24 hours, probes were perfused at 1 μL/min with artificial cerebrospinal fluid (ACSF: 147 mM NaCl, 2.2 mM $CaCl_2$, 4 mM KCl; pH 7.2) by a Harvard Apparatus (Holliston, MA, USA) infusion pump.

After an equilibration period of 60 min, dialysated samples were collected every 20 or 30 min depending on the route of D-Asp administration (acute or chronic), and were then analyzed for D-Asp, L-Asp and L-Glu content as detailed below. Conversely, samples collected in the absence of calcium were obtained by perfusing with Ca^{2+}-free ACSF solution. Olanzapine was dissolved in distilled water and administered i.p. (5 mg/kg) for 4 weeks. Chronic treatments with olanzapine or D-Asp were interrupted 24 hours before microdialysis.

5.14 High-performance liquid chromatography analysis

Dialysates were analyzed for D-Asp, L-Asp and L-Glu content by high-performance liquid chromatography (HPLC) coupled with a fluorimetric detection method as previously described (Guida et al., 2015). In this case, the HPLC system comprised a Varian ternary pump (mod. 9010), a C18 reverse-phase column, a Varian refrigerated autoinjector (mod. 9100), a Varian fluorimetric detector. Dialysates were precolumn derivatized with OPA (10 µL dialysate + 10 µL OPA) and amino acid conjugates resolved using a gradient separation. The mobile phase consisted of 2 components: a) 0.2 M sodium phosphate buffer pH 5.8, 0.1 M citric acid, and b) 90% acetonitrile, 10% distilled water. Additionally, to determine the peak area corresponding to D-Asp, selected samples were incubated in parallel with 20 µg of recombinant beef DDO for 15 min at 37 °C and analyzed as above. The disappearance/reduction of the area of D-Asp elution peak confirmed the presence of D-Asp and gave the exact D-Asp content. Data were collected by a Dell Corporation PC system 310 interfaced by Varian Star 6.2 control data and acquisition software. D-Asp and L-Asp total content in PFC homogenates was accomplished as previously reported (Topo et al., 2010), with minor modifications. Tissue samples were homogenized in 1:20 (w/v) 0.2 M TCA, sonicated (3 cycles, 10 s each) and centrifuged at 10000 g for 10 min. The precipitated protein pellets were stored at -80 °C for protein quantification, while the supernatants were neutralized with NaOH, derivatized with OPA/NAC and analyzed on a Symmetry C8 5 µm, 4.6x250 mm column (Waters, Milford, MA, USA). Identification and quantification of D-Asp and L-Asp, was based

on retention times and peak areas, compared with those associated with external standards. The identity of D-Asp and L-Asp peaks was confirmed either by the addition of internal standards, and by a pre-column treatment with RgDAAO M213R variant (which is active on acidic D-amino acids) (Sacchi et al., 2002) and StLASPO (active on L-Asp) (Bifulco et al., 2013), respectively: the samples were added with 10 µg of the enzymes, incubated at 30 °C for 30 min and then derivatized. Calibration curves were built by injecting increasing amount of standards (0.25-50 pmoles). Total protein content of PFC homogenates was determined by using the Bradford assay method, after resolubilization of the TCA precipitated protein pellets. The detected D-Asp and L-Asp total concentration in PFC homogenates was normalized by the total protein content; whereas amino acids extracellular levels were expressed as nM or µM concentration.

5.15 Synaptosomes preparation

Synaptosomes were isolated from the mouse frontal cortex as previously described (Marti et al., 2003; Mela et al., 2004; Cristino et al., 2015). The synaptosomal pellet was resuspended in oxygenated (95% O_2, 5% CO_2) Krebs solution (mM: NaCl 118.5, KCl 4.7, $CaCl_2$ 1.2, $MgSO_4$ 1.2, KH_2PO_4 1.2, $NaHCO_3$ 25, glucose 10). One mL aliquot of the suspension (~0.35 mg protein) was slowly injected into nylon syringe filters (outer diameter 13 mm, 0.45 µM pore size, internal volume of about 100 µL; Teknokroma, Barcelona, Spain) connected to a peristaltic pump. Filters were maintained at 36.5 °C, connected to a peristaltic pump and superfused at a flow rate of 0.4 mL/min with a pre-oxygenated Krebs solution containing the excitatory amino acid transporter inhibitor DL-threo-β-benzyloxyaspartic acid (TBOA, 10 µM), to prevent L-Glu release from transport reversal. Sample collection (every 3 min) was initiated after a 20 min period of filter washout. The effects of D -Asp (10 µM), L-Asp (10 µM) and NMDA (10 µM) were evaluated on 15 mM K^+-stimulated (90 s pulse) neurotransmitter outflow. Agonists were added to the perfusion medium 3 min prior to K^+ and maintained in the perfusion fluid for an additional 3 min. The NMDAR antagonist MK-801 (10 µM), the AMPA/kainate receptor antagonist CNQX (0.3 µM) and the mGlu5 receptor (mGluR5) negative allosteric modulator MTEP (0.3 µM) were perfused 3 min prior to agonists and maintained until the end of experiment.

5.16 Enzymes and inhibition assays

Recombinant M213R variant of *Rhodotorula gracilis* D-amino acid oxidase (referred to as RgDAAO; EC 1.4.3.3) and *Sulfolobus tokodaii* L-aspartate oxidase (referred to as StLASPO; EC 1.4.3.16) were overexpressed in *E. coli* cells and purified as previously described (Sacchi et al., 2002; Bifulco et al., 2013). The final M213R RgDAAO and StLASPO preparations had a specific activity of 5.8 U/mg protein on D-Asp and 0.9 U/mg protein on L-Asp, respectively. Recombinant DDO (EC 1.4.3.1) from beef kidney was expressed in *E. coli* and the purified preparation showed a specific activity of 5 U/mg protein on D-Asp (Negri et al., 1999). These flavoenzymes were fully inactive on the opposite enantiomers. Recombinant D-aspartate oxidase from mouse (mDDO) and human (hDDO) origin were overexpressed in *E. coli* cells and purified as previously reported (Katane et al., 2015), with minor modifications. The effect of olanzapine and clozapine on DDO activity was evaluated by using a coupled enzyme assay and the Amplex UltraRed reagent (Life technologies, Carlsbad, CA USA) as previously described (Hopkins et al., 2013; Terry-Lorenzo et al., 2014). In details, 0.17 U/mL of mDDO or hDDO and 0.1 U/mL horseradish peroxidase (Roche, Basel, Switzerland) were incubated for 30 min with olanzapine or clozapine (0 - 320 μM) in the presence of exogenous FAD (4 or 100 μM) in 50 mM sodium phosphate, pH 7.4, 0.06 mg/mL human serum albumin, 0.8% (w/v) DMSO; then D-Asp (7.5 mM) and the Amplex UltraRed reagent (35 μM) were added and reaction proceeded for 30 min. The fluorescence of oxidized Amplex UltraRed produced by DDO activity was measured in endpoint mode (using 540 and 595 nm as excitation and emission wavelengths, respectively). All enzymatic assays were conducted at room temperature in 96-well plate format using an automated liquid-handler system (epMotion 5075; Eppendorf, Hamburg, Germany). Data were fit to a standard, four parameters equation to determine curve top, bottom, concentration producing 50% inhibition (IC50) and Hill slope (Hopkins et al., 2013; Terry-Lorenzo et al., 2014).

6. Bibliography

Adachi M, Koyama H, Long Z, Sekine M, Furuchi T, Imai K, Nimura N, Shimamoto K, Nakajima T, Homma H (2004) L-Glutamate in the extracellular space regulates endogenous D-aspartate homeostasis in rat pheochromocytoma MPT1 cells. Arch Biochem Biophys 424:89-96.

Allen RM, Young SJ (1978) Phencyclidine-induced psychosis. Am J Psychiatry 135:1081-1084.

Amery L, Brees C, Baes M, Setoyama C, Miura R, Mannaerts GP, Van Veldhoven PP (1998) C-terminal tripeptide Ser-Asn-Leu (SNL) of human D-aspartate oxidase is a functional peroxisome-targeting signal. Biochem J 336 (Pt 2):367-371.

Anderson CM, Bridges RJ, Chamberlin AR, Shimamoto K, Yasuda-Kamatani Y, Swanson RA (2001) Differing effects of substrate and non-substrate transport inhibitors on glutamate uptake reversal. Journal of neurochemistry 79:1207-1216.

Bak LK, Schousboe A, Waagepetersen HS (2003) Characterization of depolarization-coupled release of glutamate from cultured mouse cerebellar granule cells using DL-threo-beta-benzyloxyaspartate (DL-TBOA) to distinguish between the vesicular and cytoplasmic pools. Neurochemistry international 43:417-424.

Bakshi VP, Geyer MA (1995) Antagonism of phencyclidine-induced deficits in prepulse inhibition by the putative atypical antipsychotic olanzapine. Psychopharmacology (Berl) 122:198-201.

Balu DT, Coyle JT (2012) Neuronal D-serine regulates dendritic architecture in the somatosensory cortex. Neurosci Lett 517:77-81.

Balu DT, Coyle JT (2015) The NMDA receptor 'glycine modulatory site' in schizophrenia: D-serine, glycine, and beyond. Curr Opin Pharmacol 20:109-115.

Balu DT, Li Y, Puhl MD, Benneyworth MA, Basu AC, Takagi S, Bolshakov VY, Coyle JT (2013) Multiple risk pathways for schizophrenia converge in serine racemase knockout mice, a mouse model of NMDA receptor hypofunction. Proc Natl Acad Sci U S A 110:E2400-2409.

Beard ME (1990) D-aspartate oxidation by rat and bovine renal peroxisomes: an electron microscopic cytochemical study. J Histochem Cytochem 38:1377-1381.

Bifone A, Gozzi A (2012) Neuromapping techniques in drug discovery: pharmacological MRI for the assessment of novel antipsychotics. Expert Opin Drug Discov 7:1071-1082.

Bifulco D, Pollegioni L, Tessaro D, Servi S, Molla G (2013) A thermostable L-aspartate oxidase: a new tool for biotechnological applications. Appl Microbiol Biotechnol 97:7285-7295.

Billard JM (2012) D-Amino acids in brain neurotransmission and synaptic plasticity. Amino Acids 43:1851-1860.

Calabresi P, Pisani A, Mercuri NB, Bernardi G (1992) Long-term Potentiation in the Striatum is Unmasked by Removing the Voltage-dependent Magnesium Block of NMDA Receptor Channels. The European journal of neuroscience 4:929-935.

Carli M, Calcagno E, Mainolfi P, Mainini E, Invernizzi RW (2011) Effects of aripiprazole, olanzapine, and haloperidol in a model of cognitive deficit of schizophrenia in rats: relationship with glutamate release in the medial prefrontal cortex. Psychopharmacology (Berl) 214:639-652.

Cascella NG, Macciardi F, Cavallini C, Smeraldi E (1994) d-cycloserine adjuvant therapy to conventional neuroleptic treatment in schizophrenia: an open-label study. J Neural Transm Gen Sect 95:105-111.

Cava F, Lam H, de Pedro MA, Waldor MK (2011) Emerging knowledge of regulatory roles of D-amino acids in bacteria. Cell Mol Life Sci 68:817-831.

Centonze D, Usiello A, Costa C, Picconi B, Erbs E, Bernardi G, Borrelli E, Calabresi P (2004) Chronic haloperidol promotes corticostriatal long-term potentiation by targeting dopamine D2L receptors. J Neurosci 24:8214-8222.

Centonze D, Rossi S, Tortiglione A, Picconi B, Prosperetti C, De Chiara V, Bernardi G, Calabresi P (2007) Synaptic plasticity during recovery from permanent occlusion of the middle cerebral artery. Neurobiol Dis 27:44-53.

Collingridge GL, Volianskis A, Bannister N, France G, Hanna L, Mercier M, Tidball P, Fang G, Irvine MW, Costa BM, Monaghan DT, Bortolotto ZA, Molnar E, Lodge D, Jane DE (2013) The NMDA receptor as a target for cognitive enhancement. Neuropharmacology 64:13-26.

Corrigan JJ (1969) D-amino acids in animals. Science (New York, NY 164:142-149.

Costa-Mattioli M, Sossin WS, Klann E, Sonenberg N (2009) Translational control of long-lasting synaptic plasticity and memory. Neuron 61:10-26.

Coyle JT (2012) NMDA receptor and schizophrenia: a brief history. Schizophr Bull 38:920-926.

Coyle JT, Tsai G, Goff DC (2002) Ionotropic glutamate receptors as therapeutic targets in schizophrenia. Curr Drug Targets CNS Neurol Disord 1:183-189.

Cristino L, Luongo L, Squillace M, Paolone G, Mango D, Piccinin S, Zianni E, Imperatore R, Iannotta M, Longo F, Errico F, Vescovi AL, Morari M, Maione S, Gardoni F, Nistico R, Usiello A (2015) d-Aspartate oxidase influences glutamatergic system homeostasis in mammalian brain. Neurobiol Aging 36:1890-1902.

Cull-Candy SG, Leszkiewicz DN (2004) Role of distinct NMDA receptor subtypes at central synapses. Sci STKE 2004:re16.

D'Amelio M, Cavallucci V, Middei S, Marchetti C, Pacioni S, Ferri A, Diamantini A, De Zio D, Carrara P, Battistini L, Moreno S, Bacci A, Ammassari-Teule M, Marie H, Cecconi F (2011) Caspase-3 triggers early synaptic dysfunction in a mouse model of Alzheimer's disease. Nat Neurosci 14:69-76.

D'Aniello A (2007) D-Aspartic acid: an endogenous amino acid with an important neuroendocrine role. Brain Res Rev 53:215-234.

D'Aniello A, Vetere A, Petrucelli L (1993) Further study on the specificity of D-amino acid oxidase and D-aspartate oxidase and time course for complete oxidation of D-amino acids. Comp Biochem Physiol B 105:731-734.

D'Aniello G, Tolino A, D'Aniello A, Errico F, Fisher GH, Di Fiore MM (2000) The role of D-aspartic acid and N-methyl-D-aspartic acid in the regulation of prolactin release. Endocrinology 141:3862-3870.

D'Aniello S, Spinelli P, Ferrandino G, Peterson K, Tsesarskia M, Fisher G, D'Aniello A (2005) Cephalopod vision involves dicarboxylic amino acids: D-aspartate, L-aspartate and L-glutamate. Biochem J 386:331-340.

Davies LP, Johnston GA (1976) Uptake and release of D- and L-aspartate by rat brain slices. J Neurochem 26:1007-1014.

de Bartolomeis A, Sarappa C, Magara S, Iasevoli F (2012) Targeting glutamate system for novel antipsychotic approaches: relevance for residual psychotic symptoms and treatment resistant schizophrenia. Eur J Pharmacol 682:1-11.

De Simoni S, Schwarz AJ, O'Daly OG, Marquand AF, Brittain C, Gonzales C, Stephenson S, Williams SC, Mehta MA (2013) Test-retest reliability of the BOLD pharmacological MRI response to ketamine in healthy volunteers. Neuroimage 64:75-90.

Dingledine R, Borges K, Bowie D, Traynelis SF (1999) The glutamate receptor ion channels. Pharmacol Rev 51:7-61.

Dodero L, Damiano M, Galbusera A, Bifone A, Tsaftsaris SA, Scattoni ML, Gozzi A (2013) Neuroimaging evidence of major morpho-anatomical and functional abnormalities in the BTBR T+TF/J mouse model of autism. PLoS One 8:e76655.

Domino EF (1964) Neurobiology of Phencyclidine (Sernyl), a Drug with an Unusual Spectrum of Pharmacological Activity. Int Rev Neurobiol 6:303-347.

Doyle OM, De Simoni S, Schwarz AJ, Brittain C, O'Daly OG, Williams SC, Mehta MA (2013) Quantifying the attenuation of the ketamine pharmacological magnetic resonance imaging response in humans: a validation using antipsychotic and glutamatergic agents. J Pharmacol Exp Ther 345:151-160.

Dracheva S, Marras SA, Elhakem SL, Kramer FR, Davis KL, Haroutunian V (2001) N-methyl-D-aspartic acid receptor expression in the dorsolateral prefrontal cortex of elderly patients with schizophrenia. Am J Psychiatry 158:1400-1410.

Duncan GE, Zorn S, Lieberman JA (1999) Mechanisms of typical and atypical antipsychotic drug action in relation to dopamine and NMDA receptor hypofunction hypotheses of schizophrenia. Mol Psychiatry 4:418-428.

Dunlop DS, Neidle A, McHale D, Dunlop DM, Lajtha A (1986) The presence of free D-aspartic acid in rodents and man. Biochem Biophys Res Commun 141:27-32.

Errico F, Napolitano F, Nistico R, Usiello A (2012) New insights on the role of free D-aspartate in the mammalian brain. Amino Acids 43:1861-1871.

Errico F, Pirro MT, Affuso A, Spinelli P, De Felice M, D'Aniello A, Di Lauro R (2006) A physiological mechanism to regulate D-aspartic acid and NMDA levels in mammals revealed by D-aspartate oxidase deficient mice. Gene 374:50-57.

Errico F, Rossi S, Napolitano F, Catuogno V, Topo E, Fisone G, D'Aniello A, Centonze D, Usiello A (2008a) D-aspartate prevents corticostriatal long-term depression and attenuates schizophrenia-like symptoms induced by amphetamine and MK-801. J Neurosci 28:10404-10414.

Errico F, Nistico R, Napolitano F, Oliva AB, Romano R, Barbieri F, Florio T, Russo C, Mercuri NB, Usiello A (2011a) Persistent increase of D-aspartate in D-aspartate oxidase mutant mice induces a precocious hippocampal age-dependent synaptic plasticity and spatial memory decay. Neurobiol Aging 32:2061-2074.

Errico F, Nistico R, Napolitano F, Mazzola C, Astone D, Pisapia T, Giustizieri M, D'Aniello A, Mercuri NB, Usiello A (2011b) Increased D-aspartate brain

content rescues hippocampal age-related synaptic plasticity deterioration of mice. Neurobiol Aging 32:2229-2243.

Errico F, Nistico R, Palma G, Federici M, Affuso A, Brilli E, Topo E, Centonze D, Bernardi G, Bozzi Y, D'Aniello A, Di Lauro R, Mercuri NB, Usiello A (2008b) Increased levels of d-aspartate in the hippocampus enhance LTP but do not facilitate cognitive flexibility. Mol Cell Neurosci 37:236-246.

Errico F, Santini E, Migliarini S, Borgkvist A, Centonze D, Nasti V, Carta M, De Chiara V, Prosperetti C, Spano D, Herve D, Pasqualetti M, Di Lauro R, Fisone G, Usiello A (2008c) The GTP-binding protein Rhes modulates dopamine signalling in striatal medium spiny neurons. Mol Cell Neurosci 37:335-345.

Errico F, Bonito-Oliva A, Bagetta V, Vitucci D, Romano R, Zianni E, Napolitano F, Marinucci S, Di Luca M, Calabresi P, Fisone G, Carta M, Picconi B, Gardoni F, Usiello A (2011c) Higher free D-aspartate and N-methyl-D-aspartate levels prevent striatal depotentiation and anticipate L-DOPA-induced dyskinesia. Exp Neurol 232:240-250.

Fagg GE, Matus A (1984) Selective association of N-methyl aspartate and quisqualate types of L-glutamate receptor with brain postsynaptic densities. Proc Natl Acad Sci U S A 81:6876-6880.

Fatemi SH, Folsom TD (2009) The neurodevelopmental hypothesis of schizophrenia, revisited. Schizophr Bull 35:528-548.

Ferrari L, Turrini G, Crestan V, Bertani S, Cristofori P, Bifone A, Gozzi A (2012) A robust experimental protocol for pharmacological fMRI in rats and mice. J Neurosci Methods 204:9-18.

Fujii N (2002) D-amino acids in living higher organisms. Orig Life Evol Biosph 32:103-127.

Fujii N (2005) D-amino acid in elderly tissues. Biol Pharm Bull 28:1585-1589.

Furuchi T, Homma H (2005) Free D-aspartate in mammals. Biological & pharmaceutical bulletin 28:1566-1570.

Glantz LA, Lewis DA (2000) Decreased dendritic spine density on prefrontal cortical pyramidal neurons in schizophrenia. Arch Gen Psychiatry 57:65-73.

Goff DC, Coyle JT (2001) The emerging role of glutamate in the pathophysiology and treatment of schizophrenia. Am J Psychiatry 158:1367-1377.

Goff DC, Tsai G, Manoach DS, Coyle JT (1995) Dose-finding trial of D-cycloserine added to neuroleptics for negative symptoms in schizophrenia. Am J Psychiatry 152:1213-1215.

Goff DC, Hennen J, Lyoo IK, Tsai G, Wald LL, Evins AE, Yurgelun-Todd DA, Renshaw PF (2002) Modulation of brain and serum glutamatergic concentrations following a switch from conventional neuroleptics to olanzapine. Biol Psychiatry 51:493-497.

Gong XQ, Frandsen A, Lu WY, Wan Y, Zabek RL, Pickering DS, Bai D (2005) D-aspartate and NMDA, but not L-aspartate, block AMPA receptors in rat hippocampal neurons. Br J Pharmacol 145:449-459.

Gottesman, II, Gould TD (2003) The endophenotype concept in psychiatry: etymology and strategic intentions. Am J Psychiatry 160:636-645.

Gozzi A, Schwarz A, Crestan V, Bifone A (2008a) Drug-anaesthetic interaction in phMRI: the case of the psychotomimetic agent phencyclidine. Magn Reson Imaging 26:999-1006.

Gozzi A, Large CH, Schwarz A, Bertani S, Crestan V, Bifone A (2008b) Differential effects of antipsychotic and glutamatergic agents on the phMRI response to phencyclidine. Neuropsychopharmacology 33:1690-1703.

Gozzi A, Herdon H, Schwarz A, Bertani S, Crestan V, Turrini G, Bifone A (2008c) Pharmacological stimulation of NMDA receptors via co-agonist site suppresses fMRI response to phencyclidine in the rat. Psychopharmacology (Berl) 201:273-284.

Guida F, Luongo L, Marmo F, Romano R, Iannotta M, Napolitano F, Belardo C, Marabese I, D'Aniello A, De Gregorio D, Rossi F, Piscitelli F, Lattanzi R, de Bartolomeis A, Usiello A, Di Marzo V, de Novellis V, Maione S (2015) Palmitoylethanolamide reduces pain-related behaviors and restores glutamatergic synapses homeostasis in the medial prefrontal cortex of neuropathic mice. Mol Brain 8:47.

Hardingham GE, Bading H (2010) Synaptic versus extrasynaptic NMDA receptor signalling: implications for neurodegenerative disorders. Nat Rev Neurosci 11:682-696.

Hashimoto A, Oka T (1997) Free D-aspartate and D-serine in the mammalian brain and periphery. Prog Neurobiol 52:325-353.

Hashimoto A, Oka T, Nishikawa T (1995) Anatomical distribution and postnatal changes in endogenous free D-aspartate and D-serine in rat brain and periphery. Eur J Neurosci 7:1657-1663.

Hashimoto A, Nishikawa T, Oka T, Takahashi K, Hayashi T (1992a) Determination of free amino acid enantiomers in rat brain and serum by high-performance liquid chromatography after derivatization with N-tert.-butyloxycarbonyl-L-cysteine and o-phthaldialdehyde. J Chromatogr 582:41-48.

Hashimoto A, Nishikawa T, Hayashi T, Fujii N, Harada K, Oka T, Takahashi K (1992b) The presence of free D-serine in rat brain. FEBS Lett 296:33-36.

Hashimoto A, Kumashiro S, Nishikawa T, Oka T, Takahashi K, Mito T, Takashima S, Doi N, Mizutani Y, Yamazaki T, et al. (1993) Embryonic development and postnatal changes in free D-aspartate and D-serine in the human prefrontal cortex. J Neurochem 61:348-351.

Hashimoto K, Malchow B, Falkai P, Schmitt A (2013) Glutamate modulators as potential therapeutic drugs in schizophrenia and affective disorders. Eur Arch Psychiatry Clin Neurosci 263:367-377.

Hashimoto K, Engberg G, Shimizu E, Nordin C, Lindstrom LH, Iyo M (2005) Reduced D-serine to total serine ratio in the cerebrospinal fluid of drug naive schizophrenic patients. Prog Neuropsychopharmacol Biol Psychiatry 29:767-769.

Hashimoto K, Fukushima T, Shimizu E, Komatsu N, Watanabe H, Shinoda N, Nakazato M, Kumakiri C, Okada S, Hasegawa H, Imai K, Iyo M (2003) Decreased serum levels of D-serine in patients with schizophrenia: evidence in support of the N-methyl-D-aspartate receptor hypofunction hypothesis of schizophrenia. Arch Gen Psychiatry 60:572-576.

Heresco-Levy U, Ermilov M, Shimoni J, Shapira B, Silipo G, Javitt DC (2002) Placebo-controlled trial of D-cycloserine added to conventional neuroleptics, olanzapine, or risperidone in schizophrenia. Am J Psychiatry 159:480-482.

Homma H (2007) Biochemistry of D-aspartate in mammalian cells. Amino Acids 32:3-11.

Hopkins SC et al. (2013) Structural, kinetic, and pharmacodynamic mechanisms of D-amino acid oxidase inhibition by small molecules. J Med Chem 56:3710-3724.

Horio M, Ishima T, Fujita Y, Inoue R, Mori H, Hashimoto K (2013) Decreased levels of free D-aspartic acid in the forebrain of serine racemase (Srr) knock-out mice. Neurochemistry international 62:843-847.

Howes OD, Kapur S (2009) The dopamine hypothesis of schizophrenia: version III--the final common pathway. Schizophr Bull 35:549-562.

Huang AS, Beigneux A, Weil ZM, Kim PM, Molliver ME, Blackshaw S, Nelson RJ, Young SG, Snyder SH (2006) D-aspartate regulates melanocortin formation and function: behavioral alterations in D-aspartate oxidase-deficient mice. J Neurosci 26:2814-2819.

Huang W, Zhu PJ, Zhang S, Zhou H, Stoica L, Galiano M, Krnjevic K, Roman G, Costa-Mattioli M (2013) mTORC2 controls actin polymerization required for consolidation of long-term memory. Nat Neurosci 16:441-448.

Ikonomidou C, Bittigau P, Koch C, Genz K, Hoerster F, Felderhoff-Mueser U, Tenkova T, Dikranian K, Olney JW (2001) Neurotransmitters and apoptosis in the developing brain. Biochem Pharmacol 62:401-405.

Javitt DC (1987) Negative schizophrenic symptomatology and the PCP (phencyclidine) model of schizophrenia. Hillside J Clin Psychiatry 9:12-35.

Javitt DC (2004) Glutamate as a therapeutic target in psychiatric disorders. Mol Psychiatry 9:984-997, 979.

Javitt DC (2012) Twenty-five years of glutamate in schizophrenia: are we there yet? Schizophr Bull 38:911-913.

Javitt DC, Zukin SR (1991) Recent advances in the phencyclidine model of schizophrenia. Am J Psychiatry 148:1301-1308.

Javitt DC, Zukin SR, Heresco-Levy U, Umbricht D (2012) Has an angel shown the way? Etiological and therapeutic implications of the PCP/NMDA model of schizophrenia. Schizophr Bull 38:958-966.

Javitt DC, Zylberman I, Zukin SR, Heresco-Levy U, Lindenmayer JP (1994) Amelioration of negative symptoms in schizophrenia by glycine. Am J Psychiatry 151:1234-1236.

Jones CA, Watson DJ, Fone KC (2011) Animal models of schizophrenia. Br J Pharmacol 164:1162-1194.

Kalia LV, Kalia SK, Salter MW (2008) NMDA receptors in clinical neurology: excitatory times ahead. Lancet Neurol 7:742-755.

Katane M, Homma H (2010) D-aspartate oxidase: the sole catabolic enzyme acting on free D-aspartate in mammals. Chem Biodivers 7:1435-1449.

Katane M, Homma H (2011) D-Aspartate--an important bioactive substance in mammals: a review from an analytical and biological point of view. J Chromatogr B Analyt Technol Biomed Life Sci 879:3108-3121.

Katane M, Yamada S, Kawaguchi G, Chinen M, Matsumura M, Ando T, Doi I, Nakayama K, Kaneko Y, Matsuda S, Saitoh Y, Miyamoto T, Sekine M, Yamaotsu N, Hirono S, Homma H (2015) Identification of Novel D-Aspartate Oxidase Inhibitors by in Silico Screening and Their Functional and Structural Characterization in Vitro. J Med Chem 58:7328-7340.

Kim PM, Duan X, Huang AS, Liu CY, Ming GL, Song H, Snyder SH (2010) Aspartate racemase, generating neuronal D-aspartate, regulates adult neurogenesis. Proc Natl Acad Sci U S A 107:3175-3179.

Koyama H, Adachi M, Sekine M, Katane M, Furuchi T, Homma H (2006) Cytoplasmic localization and efflux of endogenous D-aspartate in pheochromocytoma 12 cells. Arch Biochem Biophys 446:131-139.

Krashia P, Ledonne A, Nobili A, Cordella A, Errico F, Usiello A, D'Amelio M, Mercuri NB, Guatteo E, Carunchio I (2015) Persistent elevation of D-Aspartate enhances NMDA receptor-mediated responses in mouse substantia nigra pars compacta dopamine neurons. Neuropharmacology 103:69-78.

Krebs HA (1935) Metabolism of amino-acids: Deamination of amino-acids. Biochem J 29:1620-1644.

Kulkarni VA, Firestein BL (2012) The dendritic tree and brain disorders. Mol Cell Neurosci 50:10-20.

Labrie V, Wong AH, Roder JC (2012) Contributions of the D-serine pathway to schizophrenia. Neuropharmacology 62:1484-1503.

Lamprecht R, LeDoux J (2004) Structural plasticity and memory. Nat Rev Neurosci 5:45-54.

Long Z, Homma H, Lee JA, Fukushima T, Santa T, Iwatsubo T, Yamada R, Imai K (1998) Biosynthesis of D-aspartate in mammalian cells. FEBS Lett 434:231-235.

Malthe-Sorenssen D, Skrede KK, Fonnum F (1979) Calcium-dependent release of D-[3H]aspartate evoked by selective electrical stimulation of excitatory afferent fibres to hippocampal pyramidal cells in vitro. Neuroscience 4:1255-1263.

Marti M, Mela F, Ulazzi L, Hanau S, Stocchi S, Paganini F, Beani L, Bianchi C, Morari M (2003) Differential responsiveness of rat striatal nerve endings to the mitochondrial toxin 3-nitropropionic acid: implications for Huntington's disease. Eur J Neurosci 18:759-767.

Martineau M, Baux G, Mothet JP (2006) D-serine signalling in the brain: friend and foe. Trends Neurosci 29:481-491.

Matsuzaki M, Honkura N, Ellis-Davies GC, Kasai H (2004) Structural basis of long-term potentiation in single dendritic spines. Nature 429:761-766.

Mela F, Marti M, Ulazzi L, Vaccari E, Zucchini S, Trapella C, Salvadori S, Beani L, Bianchi C, Morari M (2004) Pharmacological profile of nociceptin/orphanin FQ receptors regulating 5-hydroxytryptamine release in the mouse neocortex. Eur J Neurosci 19:1317-1324.

Millan MJ (2002) N-methyl-D-aspartate receptor-coupled glycineB receptors in the pathogenesis and treatment of schizophrenia: a critical review. Curr Drug Targets CNS Neurol Disord 1:191-213.

Moghaddam B, Krystal JH (2012) Capturing the angel in "angel dust": twenty years of translational neuroscience studies of NMDA receptor antagonists in animals and humans. Schizophr Bull 38:942-949.

Molinaro G, Pietracupa S, Di Menna L, Pescatori L, Usiello A, Battaglia G, Nicoletti F, Bruno V (2010) D-aspartate activates mGlu receptors coupled to polyphosphoinositide hydrolysis in neonate rat brain slices. Neurosci Lett 478:128-130.

Monahan JB, Michel J (1987) Identification and characterization of an N-methyl-D-aspartate-specific L-[3H]glutamate recognition site in synaptic plasma membranes. J Neurochem 48:1699-1708.

Morris BJ, Cochran SM, Pratt JA (2005) PCP: from pharmacology to modelling schizophrenia. Curr Opin Pharmacol 5:101-106.

Nacher J, McEwen BS (2006) The role of N-methyl-D-asparate receptors in neurogenesis. Hippocampus 16:267-270.

Nakatsuka S, Hayashi M, Muroyama A, Otsuka M, Kozaki S, Yamada H, Moriyama Y (2001) D-Aspartate is stored in secretory granules and released through a Ca(2+)-dependent pathway in a subset of rat pheochromocytoma PC12 cells. J Biol Chem 276:26589-26596.

Negri A, Tedeschi G, Ceciliani F, Ronchi S (1999) Purification of beef kidney D-aspartate oxidase overexpressed in Escherichia coli and characterization of its redox potentials and oxidative activity towards agonists and antagonists of excitatory amino acid receptors. Biochim Biophys Acta 1431:212-222.

Negri A, Ceciliani F, Tedeschi G, Simonic T, Ronchi S (1992) The primary structure of the flavoprotein D-aspartate oxidase from beef kidney. J Biol Chem 267:11865-11871.

Neidle A, Dunlop DS (1990) Developmental changes in free D-aspartic acid in the chicken embryo and in the neonatal rat. Life Sci 46:1517-1522.

Nistico R, Pignatelli M, Piccinin S, Mercuri NB, Collingridge G (2012) Targeting synaptic dysfunction in Alzheimer's disease therapy. Mol Neurobiol 46:572-587.

Ogita K, Yoneda Y (1988) Disclosure by triton X-100 of NMDA-sensitive [3H] glutamate binding sites in brain synaptic membranes. Biochem Biophys Res Commun 153:510-517.

Okamoto K, Nagai T, Miyawaki A, Hayashi Y (2004) Rapid and persistent modulation of actin dynamics regulates postsynaptic reorganization underlying bidirectional plasticity. Nat Neurosci 7:1104-1112.

Olverman HJ, Jones AW, Mewett KN, Watkins JC (1988) Structure/activity relations of N-methyl-D-aspartate receptor ligands as studied by their inhibition of [3H]D-2-amino-5-phosphonopentanoic acid binding in rat brain membranes. Neuroscience 26:17-31.

Owen MJ, O'Donovan MC, Thapar A, Craddock N (2011) Neurodevelopmental hypothesis of schizophrenia. Br J Psychiatry 198:173-175.

Palacin M, Estevez R, Bertran J, Zorzano A (1998) Molecular biology of mammalian plasma membrane amino acid transporters. Physiol Rev 78:969-1054.

Pollegioni L, Piubelli L, Sacchi S, Pilone MS, Molla G (2007) Physiological functions of D-amino acid oxidases: from yeast to humans. Cell Mol Life Sci 64:1373-1394.

Punzo D, Errico F, Cristino L, Sacchi S, Keller S, Belardo C, Luongo L, Nuzzo T, Imperatore R, Florio E, De Novellis V, Affinito O, Migliarini S, Maddaloni G, Sisalli MJ, Pasqualetti M, Pollegioni L, Maione S, Chiariotti L, Usiello A (2016) Age-Related Changes in d-Aspartate Oxidase Promoter Methylation Control Extracellular d-Aspartate Levels and Prevent Precocious Cell Death during Brain Aging. J Neurosci 36:3064-3078.

Ransom RW, Stec NL (1988) Cooperative modulation of [3H]MK-801 binding to the N-methyl-D-aspartate receptor-ion channel complex by L-glutamate, glycine, and polyamines. J Neurochem 51:830-836.

Ritter LM, Vazquez DM, Meador-Woodruff JH (2002) Ontogeny of ionotropic glutamate receptor subunit expression in the rat hippocampus. Brain Res Dev Brain Res 139:227-236.

Sacchi S, Caldinelli L, Cappelletti P, Pollegioni L, Molla G (2012) Structure-function relationships in human D-amino acid oxidase. Amino Acids 43:1833-1850.

Sacchi S, Lorenzi S, Molla G, Pilone MS, Rossetti C, Pollegioni L (2002) Engineering the substrate specificity of D-amino-acid oxidase. J Biol Chem 277:27510-27516.

Sakai K, Homma H, Lee JA, Fukushima T, Santa T, Tashiro K, Iwatsubo T, Imai K (1998) Emergence of D-aspartic acid in the differentiating neurons of the rat central nervous system. Brain research 808:65-71.

Savage DD, Galindo R, Queen SA, Paxton LL, Allan AM (2001) Characterization of electrically evoked [3H]-D-aspartate release from hippocampal slices. Neurochem Int 38:255-267.

Sawa A, Snyder SH (2003) Schizophrenia: neural mechanisms for novel therapies. Mol Med 9:3-9.

Schell MJ, Cooper OB, Snyder SH (1997) D-aspartate localizations imply neuronal and neuroendocrine roles. Proc Natl Acad Sci U S A 94:2013-2018.

Setoyama C, Miura R (1997) Structural and functional characterization of the human brain D-aspartate oxidase. J Biochem 121:798-803.

Sforazzini F, Schwarz AJ, Galbusera A, Bifone A, Gozzi A (2014) Distributed BOLD and CBV-weighted resting-state networks in the mouse brain. Neuroimage 87:403-415.

Sokolov BP (1998) Expression of NMDAR1, GluR1, GluR7, and KA1 glutamate receptor mRNAs is decreased in frontal cortex of "neuroleptic-free" schizophrenics: evidence on reversible up-regulation by typical neuroleptics. J Neurochem 71:2454-2464.

Still JL, Buell MV, et al. (1949) Studies on the cyclophorase system; D-aspartic oxidase. J Biol Chem 179:831-837.

Storm-Mathisen J, Wold JE (1981) In vivo high-affinity uptake and axonal transport of D-[2,3-3H]aspartate in excitatory neurons. Brain Res 230:427-433.

Streit P (1980) Selective retrograde labeling indicating the transmitter of neuronal pathways. J Comp Neurol 191:429-463.

Tan HY, Callicott JH, Weinberger DR (2007) Dysfunctional and compensatory prefrontal cortical systems, genes and the pathogenesis of schizophrenia. Cereb Cortex 17 Suppl 1:i171-181.

Tanaka-Hayashi A, Hayashi S, Inoue R, Ito T, Konno K, Yoshida T, Watanabe M, Yoshimura T, Mori H (2014) Is D-aspartate produced by glutamic-oxaloacetic transaminase-1 like 1 (Got1l1): a putative aspartate racemase? Amino Acids.

Tang SJ, Reis G, Kang H, Gingras AC, Sonenberg N, Schuman EM (2002) A rapamycin-sensitive signaling pathway contributes to long-term synaptic plasticity in the hippocampus. Proc Natl Acad Sci U S A 99:467-472.

Taxt T, Storm-Mathisen J (1984) Uptake of D-aspartate and L-glutamate in excitatory axon terminals in hippocampus: autoradiographic and biochemical comparison with gamma-aminobutyrate and other amino acids in normal rats and in rats with lesions. Neuroscience 11:79-100.

Terry-Lorenzo RT, Chun LE, Brown SP, Heffernan ML, Fang QK, Orsini MA, Pollegioni L, Hardy LW, Spear KL, Large TH (2014) Novel human D-amino acid oxidase inhibitors stabilize an active-site lid-open conformation. Biosci Rep 34.

Topo E, Fisher G, Sorricelli A, Errico F, Usiello A, D'Aniello A (2010) Thyroid hormones and D-aspartic acid, D-aspartate oxidase, D-aspartate racemase, H2O2, and ROS in rats and mice. Chem Biodivers 7:1467-1478.

Tsai G, Yang P, Chung LC, Lange N, Coyle JT (1998) D-serine added to antipsychotics for the treatment of schizophrenia. Biol Psychiatry 44:1081-1089.

Van Veldhoven PP, Brees C, Mannaerts GP (1991) D-aspartate oxidase, a peroxisomal enzyme in liver of rat and man. Biochim Biophys Acta 1073:203-208.

Wilkin GP, Garthwaite J, Balazs R (1982) Putative acidic amino acid transmitters in the cerebellum. II. Electron microscopic localization of transport sites. Brain Res 244:69-80.

Wolosker H, Blackshaw S, Snyder SH (1999) Serine racemase: a glial enzyme synthesizing D-serine to regulate glutamate-N-methyl-D-aspartate neurotransmission. Proc Natl Acad Sci U S A 96:13409-13414.

Wolosker H, D'Aniello A, Snyder SH (2000) D-aspartate disposition in neuronal and endocrine tissues: ontogeny, biosynthesis and release. Neuroscience 100:183-189.

Yamada K, Ohnishi T, Hashimoto K, Ohba H, Iwayama-Shigeno Y, Toyoshima M, Okuno A, Takao H, Toyota T, Minabe Y, Nakamura K, Shimizu E, Itokawa M, Mori N, Iyo M, Yoshikawa T (2005) Identification of multiple serine racemase (SRR) mRNA isoforms and genetic analyses of SRR and DAO in schizophrenia and D-serine levels. Biol Psychiatry 57:1493-1503.

Zaar K, Kost HP, Schad A, Volkl A, Baumgart E, Fahimi HD (2002) Cellular and subcellular distribution of D-aspartate oxidase in human and rat brain. J Comp Neurol 450:272-282.

Zhan Y, Paolicelli RC, Sforazzini F, Weinhard L, Bolasco G, Pagani F, Vyssotski AL, Bifone A, Gozzi A, Ragozzino D, Gross CT (2014) Deficient neuron-microglia signaling results in impaired functional brain connectivity and social behavior. Nat Neurosci 17:400-406.

7. Pubblications

Quantitative determination of D-Asp, L-Asp and N-methyl-D-Aspartate in biological fluids by chiral separation and Multiple Reaction Monitoring tandem mass spectrometry. Carolina Fontanarosa, Nunzio Sepe, **Marta Squillace**, Alessandro Usiello, Piero Pucci and Angela Amoresano. In Submission

Olanzapine but not clozapine perturbs free D-aspartate metabolism in the brain. Silvia Sacchi*, Carmela Belardo*, **Marta Squillace***, Francesco Errico*, Paolo Bolognesi, Giovanna Paolone, Elena Rosini, Zoraide Motta, Martina Frassineti, Vito De Novellis,Alessandro Bertolino, Loredano Pollegioni, Michele Morari, Sabatino Maione, Alessandro Usiello. In Submission

Exposure Of E. Coli To Dna-Methylating Agents Impairs Biofilm Formation And Invasion Of Eukaryotic Cells Via Down Regulation Of The N-Acetylneuraminate Lyase Nana. Pamela Di Pasquale, Marianna Caterino, Angela Di Somma, **Marta Squillace**, Elio Rossi, Paolo Landini, Valerio Iebba, Serena Schippa, Rosanna Papa, Laura Selan, Marco Artini, Annateresa Palamara And Angela Duilio. Frontiers In Microbiology. 7:147. Doi:10.3389/Fmicb.2016.00147

D-Aspartate-Oxidase Influences Glutamatergic System Homeostasis In Mammalian Brain. Luigia Cristino*, Livio Luongo*, **Marta Squillace***, Giovanna Paolone, Dalila Mango, Sonia Piccinin, Elisa Zianni, Roberta Imperatore, Monica Iannotta, Francesco Longo, Francesco Errico, Angelo Luigi Vescovi, Michele Morari, Sabatino Maione, Fabrizio Gardoni, Robert Nisticò, Alessandro Usiello. Neurobiology Of Aging 2015 May;36(5):1890-902. Doi: 10.1016/J.Neurobiolaging.2015.02.003. Epub 2015 Feb 12. Pmid: 25771393

A Role For D-Aspartate Oxidase In Schizophrenia And In Schizophrenia-Related Symptoms Induced By Phencyclidine In Mice. F Errico,Vd'argenio, F Sforazzini, F Iasevoli, **M Squillace**, G Guerri, F Napolitano, T Angrisano, A Di Maio,S Keller, D Vitucci, A Galbusera, L Chiariotti, A Bertolino, A De Bartolomeis, F Salvatore, A Gozzi And A Usiello. Transl Psychiatry (2015)5, E512; DOI:10.1038/TP.2015.2

D-Aspartate Modulates Nociceptive-Specific Neuron Activity And Pain Threshold In Inflammatory And Neuropathic Pain Condition In Mice. Serena Boccella, Valentina Vacca, Francesco Errico, Sara Marinelli, **Marta Squillace**, Francesca Guida, Anna Di Maio, Daniela Vitucci, Enza Palazzo, Vito De Novellis, Sabatino Maione, Flaminia Pavone, And Alessandro Usiello. Hindawi Publishing Corporation Biomed Research International Volume 2015, ARTICLE ID 905906,10 Pages HTTP://DX.DOI.ORG/10.1155/2015/905906

Dysfunctional Dopaminergic Neurotransmission In Asocial Btbr Mice. **Squillace M**, Dodero L, Federici M, Migliarini S, Errico F, Napolitano F, Krashia P, Di Maio A, Galbusera A, Bifone A, Scattoni Ml, Pasqualetti M, Mercuri Nb, Usiello A, Gozzi A. Transl Psychiatry. 2014 Aug 19;4:E427. Doi: 10.1038/Tp.2014.69.

Free D-Aspartate Regulates Neuronal Dendritic Morphology, Synaptic Plasticity, Grey Matter Volume And Brain Activity In Mammals. F Errico, R Nisticò, A Di Giorgio, **M Squillace**, D Vitucci, A Galbusera, S Piccinin, D Mango, L Fazio, S Middei, S Trizio, N B Mercuri, M Ammassari Teule, D Centonze, A Gozzi, G Blasi, A Bertolino, A Usiello. Transl Psychiatry. 2014 Jul 29;4:E417. Doi: 10.1038/Tp.2014.59.

Decreased levels of D-aspartate and NMDA in the prefrontal cortex and striatum of patients with schizophrenia. Errico F, Napolitano F, **Squillace M**, Vitucci D, Blasi G, de Bartolomeis A, Bertolino A, D'Aniello A,Usiello A. J Psychiatr Res. 2013 Oct;47(10):1432-7. doi: 10.1016/j.jpsychires.2013.06.013. Epub 2013 Jul 6.

Bimodal effect of D-aspartate on brain aging processes: insights from animal models. F. Errico, A. Di Maio, V. Marsili, **M. Squillace**, D. Vitucci, F. Napolitano, A. Usiello. Journal of Biological Regulators & Homeostatic Agents [0393-974X] 2013 vol:27 iss:2 SUPPL. pag:49 -59.

Role of D-aspartate in glutamatergic neurotransmission: new insights from animal models. F. Errico, F. Napolitano, D. Vitucci, A. Di Maio, **M. Squillace**, V. Marsili, F. Marmo, L. Chiariotti, A. Usiello. European Journal of Neurodegenerative Diseases [2279-5855] 2012 vol:1 no:2 pag: 267-274.